41. Multifunctional Plant Surfaces and Smart Materials

Kerstin Koch, Bharat Bhushan, Wilhelm Barthlott

The surfaces of plants represent multifunctional interfaces between the organisms and their biotic (living) and the nonbiotic solid, liquid, and gaseous environment. The diversity of plant surface structures has evolved over several hundred million years of evolution. Evolutionary processes have led to a large variety of functional plant surfaces which exhibit, for example, superhydrophobicity, self-cleaning, superhydrophilicity, and reduction of adhesion and light reflection. The primary surface of nearly all parts of land plants is the epidermis. The outer part of epidermal cells is an extracellular membrane called the cuticle. The cuticle, with its associated waxes, is a stabilization element, has a barrier function, and is responsible for various kinds of surface structuring by cuticular folding or deposition of three-dimensional wax crystals on the cuticle. Surface properties, such as superhydrophobicity, self-cleaning, reduction of adhesion and light reflection, and absorption of harmful ultraviolet (UV) radiation, are based on the existence of three-dimensional waxes. Waxes form different morphologies, such as tubules, platelets or rodlets, by self-assembly. The ability of plant waxes to self-assemble into three-dimensional nanostructures can be used to create hierarchical roughness of various kinds of surfaces. The structures and principles which nature uses to develop functional surfaces are of special interest in biomimetics. Hierarchical structures play a key role in surface wetting and are discussed in the context of superhydrophobic and self-cleaning plants and for the development of biomimetic surfaces. Superhydrophobic biomimetic surfaces are introduced and their use for self-cleaning or development of air-retaining surfaces, for, e.g., drag reduction at surfaces moving in water, are discussed. This chapter presents an overview of plant structures, combines the structural basis of plant surfaces with their functions, and introduces existing biomimetic superhydrophobic surfaces and their fabrication.

Plant surfaces are multifunctional interfaces between the plant and the physical and biological environment. They have developed over several million years of evolution by a long-lasting game of mutation and selection, or trial and error, for the development of adaptations to their environment. These evolutionary processes led to

huge structural variety and the development of multifunctional, protective interfaces.

Even in a cursory look at plants it is obvious that plant surfaces appear different. Surface structures on micro- and nanoscales are responsible for these different optical appearances. A selection of common plant surfaces and their surface structures, imaged by scanning electron microscopy (SEM), is shown in Fig. 41.1. Based on a microscopically smooth surface, the leaves of *Magnolia grandiflora* appear glossy (Fig. 41.1a,b). These and many other glossy leaves are covered by a thin layer of hydrophobic waxes, not or only rarely detectable in SEM images. Other leaves appear velvety, and under SEM they show a much rougher surface structure, built up by convex cells, with a nanostructure superimposed on them. Velvety surfaces are common on flower petals of roses, daisies, and *Dahlia*, as shown in Fig. 41.1c,d. A dense layer of air-filled hairs make the leaves of *Leucadendron argenteum* appear silvery (Fig. 41.1e,f). Hairy surfaces are common on all known life forms, as trees, shrubs, and herbaceous plants, but are absent in plants growing underwater. The leaves of *Eucalyptus macrocarpa* (Fig. 41.1g) and the surfaces of some fruits such as plums appear bluish because of a dense coverage of three-dimensional waxes, such as those shown in Fig. 41.1h. The waxes, hairs, and convex cells shown here are very common in plant surfaces but occur in different morphologies, which are discussed in detail in this chapter.

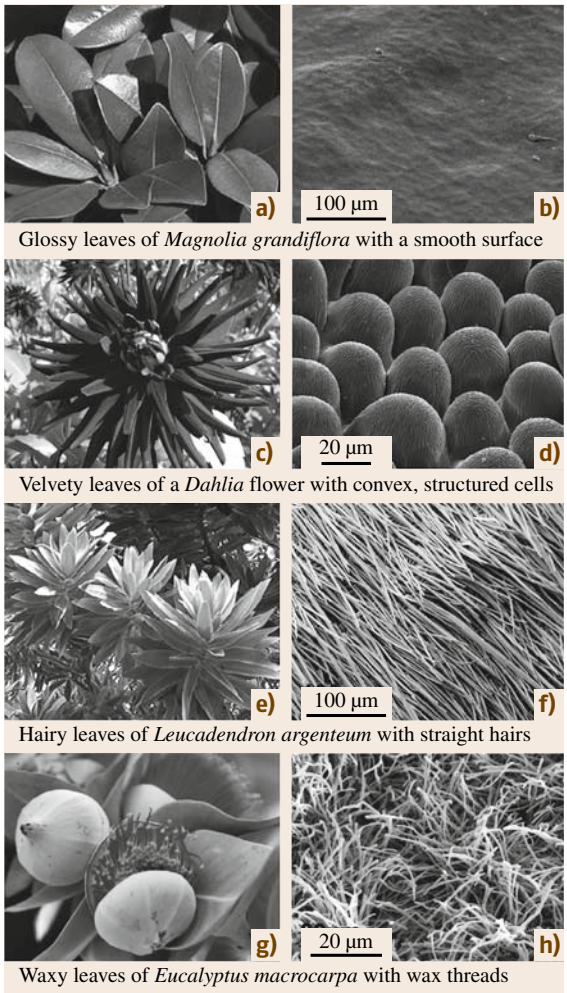

Fig. 41.1a–h Macroscopic optical appearance of plant surfaces, and their surface microstructures shown in SEM micrographs. In **(a)** leaves of *Magnolia grandiflora* appear glossy because of a flat surface structure, shown in figure **(b)**. In **(c)** the flower petals of *Dahlia* appear velvety, because of the convex microstructure of the epidermis cells, shown in **(d)**. In **(e)** the silvery appearance of *Leucadendron argenteum* leaves is caused by a dense layer of light-reflecting hairs, shown in **(f)**. In **(g)** the leaf and flower bud surfaces of *Eucalyptus macrocarpa* appear white or bluish, caused by a dense covering with three-dimensional waxes, shown in **(h)**

The diversity of plant surface structures arises from the variability of cell shapes, micro- and nanostructures of the cell surfaces, and by the formation of multicellular structures. Based on these cellular and subcellular units a nearly unlimited combination of structures leads to a large structural biodiversity of plant surfaces [41.1–4]. The epidermis, as the outermost cell layer of the primary tissues of all leaves and several other organs of plants, plays an important role in environmental interactions and surface structuring. The simplified model presented in Fig. 41.2 shows a layered stratification of the outermost part of epidermis cells. Starting with the outside, one finds a highly functional thin outermost layer, called the cuticle. This outermost layer covers nearly all aerial tissues of land-living plants as a continuous extracellular membrane, but is absent in roots. One of the most important attributes of the cuticle is its function as a transpiration barrier, which enables plants to overcome the physical and physiological problems connected to an ambient environment, such as desiccation.

The cuticle is basically a biopolymer made of a polyester called cutin, impregnated with integrated (intracuticular) waxes. Waxes on the cuticle surface (epicuticular waxes) play an important role in surface structuring at the subcellular scale. They occur in dif-

ferent morphologies, show a large variability in their chemistry, and are able to self-assemble into three-dimensional crystals. Intracuticular waxes function as the main transport barrier to reduce the loss of water and small molecules such as ions from inside the cell, and also reduce the uptake of liquids and molecules from the outside [41.5]. The next layer shown in Fig. 41.2 is the pectin layer. It connects the cuticle to the much thicker underlying cellulose wall, which is built by single cellulose fibrils. Pectin is not always formed as a layer, but in some species, especially during the early ontogeny of the cuticle, a layered structure has been shown by transmission electron microscopy. Additionally polysaccharides, not shown in this schematic, are integrated into the cellulose wall. The last layer shown is the plasma membrane, which separates the living compartment of the water-containing cell from the outer, nonliving part of the epidermis.

Plant surfaces provide multifunctional interfaces with their environments. Their properties include the reflection and adsorption of solar radiation. These properties have been optimized in plants which are exposed to intense radiation, e.g., in deserts, to reduce the uptake of harmful radiation and heat energy. The most important structural units for these functions are plant waxes and hairs [41.2]. In other plants the surfaces are optimized for the reduction of adhesion, e.g., insect adhesion. Optimized surfaces with anti-adhesive properties for insects can be found in carnivorous plants, which developed slippery surfaces to catch insects. The structural basis for slippery surfaces is given by three-dimensional waxes, which reduce adhesion by developing a sufficient surface roughness. Other surfaces reduce the adhesion of insects by providing a water film on their surfaces. In plants, we find all kinds of surface wettability. Superhydrophilicity lets water completely spread on the surface. Such surfaces have been developed in plants which use their complete surface for the uptake of water and nutrients from the environment. Therefore plants developed porous or specialized hairy surfaces. On superhydrophobic surfaces wetting is hindered since water forms spherical droplets and the contact to the surface is minimized. These properties have been developed by different groups of plants to prevent water films on the surface from reducing gas exchange and to reduce the growth of pathogenic microorganisms by maintaining a dry surface. Some plants with leaves that float on water, such as *Azolla* and *Salvinia* species, use their superhydrophobicity to stay dry, even when they are submerged in water. The structural basics of the leaf surfaces of *Azolla*

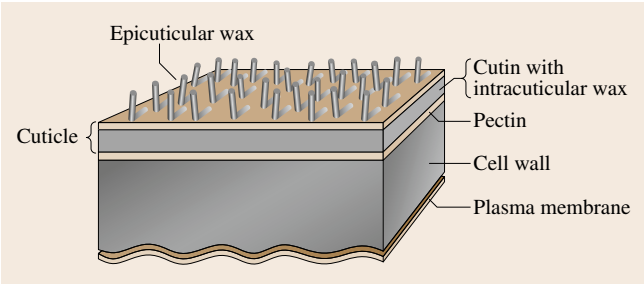

Fig. 41.2 A simplified model of the stratification of the outermost layers of plant epidermis cells. In this scheme, the outermost wax layer is shown in its commonest form, as a composite of three-dimensional waxes with an underlying wax film. Below this layer is the cuticula, made of a cutin network and integrated waxes. The cuticula is connected with the underlying cellulose wall by pectin, here simply visualized as a layer. Below the cell wall, the plasma membrane is shown. This membrane separates the water-containing part of the cells from the outermost structure-forming components of the epidermis above

and *Salvinia* are large multicellular hairs, covered with three-dimensional waxes. Some plants, such as the lotus (*Nelumbo nucifera*) leaves, have superhydrophobic surfaces which are also self-cleaning. On such surfaces, the attachment and growth of pathogens is reduced, and a water droplet rolling over the surface collects pathogens and other dirt particles and thereby cleans the surface. The superhydrophobic and self-cleaning properties of plant surfaces are always correlated with the presence of three-dimensional waxes, but are common and optimized in surfaces with convex epidermal cells [41.6].

Plant surfaces provide a large diversity of structures and functions which can be useful for the development of biomimetic surfaces and materials. In biomimetics (synonym *bionics*) a wide spectra of research fields combines biological innovations with technical approaches. Some successful biomimetic surfaces, such as water-repellent and self-cleaning surfaces, have already been developed.

The cuticle and its waxes are the most important materials used by plants to provide multifunctional properties, thus both are introduced in this chapter. Special attention is given to the epicuticular wax crystals, their diverse chemistry and morphology, and their ability to self-assemble into micro- and nanostructures. The origin and diversity of plant surface structures is based on the epidermis cells, and their shapes and surface structures. The morphological variations leading to various surface structures are introduced, and several

examples are given. The functional properties of plant surfaces are presented and correlated with their specific surface structures. In this chapter the structural basics for superhydrophobicity and its existing and potential technical uses are discussed.

SEM micrographs presented in the chapter were taken from a database of some 250 000 SEM micrographs at the University of Bonn, which has been built up as a result of 30 years of SEM research on biological surfaces by the senior author and his collaborators.

41.1 The Architecture of Plant Surfaces

41.1.1 The Plant Cuticle: a Multifunctional Interface

Approximately 460 million years ago, when the first plants moved from their aqueous environment to the drier atmosphere on land [41.8], plants needed a protective skin to survive in the drier gaseous environment. This, for most plant surfaces, is a continuous membrane, called the cuticle. The cuticle serves as a multifunctional interface of the primary tissue of all land-living plants, which have vessels for the transport of water, e.g., ferns, conifers, and flowering plants. Roots and some secondary plant tissues, such as wood and bark, are not covered by a cuticle. The cuticle is a hydrophobic composite material, made basically of a polymer called cutin, and integrated and superimposed lipids called *waxes*, which enable plants to overcome the physical and physiological problems connected with an ambient environment, such as desiccation [41.5]. The cuticle network is formed by cutin, a polyester-like biopolymer composed of hydroxyl and hydroxyepoxy fatty acids, and sometimes also by cutan, which is built by polymethylene chains. Nonlipidic compounds of the cuticle are cellulose, pectin, phenolics, and proteins. Large differences in the chemical composition and microstructure of the waxes and the cutin network have been found by comparing different species and different developmental stages of organ ontogeny. Chemical composition, microstructure, and biosynthesis of the cuticle have been reviewed by several authors [41.9–11], and a few books summarize the intensive research on plant cuticles [41.12–15].

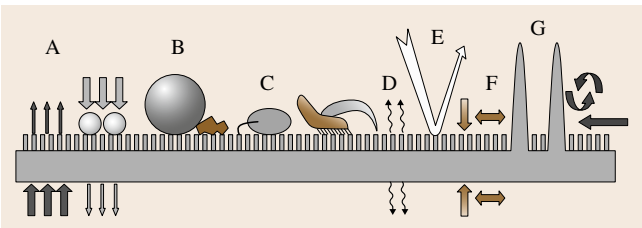

Fig. 41.3 Schematic of the most prominent functions of the plant boundary layer on a hydrophobic microstructured surface: (A) transport barrier: limitation of uncontrolled water loss/leaching from the interior and foliar uptake; (B) surface wettability; (C) antiadhesive, self-cleaning properties: reduction of contamination, pathogen attack, and attachment/locomotion of insects; (D) signaling: cues for host pathogens/insect recognition and epidermal cell development; (E) optical properties: protection against harmful radiation; (F) mechanical properties: resistance against mechanical stress and maintenance of physiological integrity, and (G) reduction of surface temperature by increasing turbulent air flow over the air boundary layer (after *Bargel* et al. [41.7])

Based on their hydrophobic chemistry and diversity of micro- and nanostructures, the cuticle provides several protective properties, which are summarized in Fig. 41.3. One of the most important properties is the function as a transpiration barrier (A in Fig. 41.3), which is based on the hydrophobic integrated and superimposed waxes. In this, the intracuticular waxes, which are located in the cutin network, form the main transport barrier to reduce the loss of water by transpiration and reduce leaching of molecules from inside the cells [41.16]. In addition to the reduction of water loss, the cuticle prevents leaching of ions from the inside of the cells to the environment and the uptake of molecules from the outside. Epi- and intracuticular waxes reduce the uptake of molecules from the environment, which might become a crucial factor in agriculture when the uptake of, e.g., nutrients or fungicides is desired. The cuticle structure, as well as chemistry, has a strong influence on the wettability (B in Fig. 41.3) and adherence of particles, pathogens, and insects (C in Fig. 41.3). The epicuticular waxes are responsible for the maintenance of wettability and self-cleaning properties [41.17, 18]. The three-dimensional waxes play an important role in surface structuring, e.g., formation of hierarchical surface, and they can reduce the adhesion of particles [41.6, 19]. These aspects are of great interest for the development of water-repellent and self-cleaning technical surfaces and will be discussed later in detail. Three-dimensional waxes not only reduce the adhesion

of particles; they also reduce the adhesion of insects. This property has been developed very efficiently by some carnivorous plants to trap insects. The structural basics of waxy and other slippery plant surfaces are introduced in Sect. 41.2. The plant cuticle also plays an important role for insect and microorganism interaction, whereby some surface structures have a signaling function (D in Fig. 41.3). In some species epicuticular waxes are responsible for reflection of visible light; others are effective in adsorption of harmful UV radiation (E in Fig. 41.3). However, there are various strategies in plants to increase light reflection. Thus, this part is also introduced in detail in Sect. 41.2. Cuticles are thin membranes, with thicknesses between a few nanometers and some micrometers, but they are an important structural stabilization component for the primary epidermis tissue (F in Fig. 41.3) [41.7], with elasticity modulus in the same range as that of technical polypropylene membranes of comparable thickness [41.20, 21]. Structural components at larger scales increase the heat transfer via induction of turbulent air flow and convection (G in Fig. 41.3). Examples of several functional surface structures are introduced in more detail later.

41.1.2 Waxes – Hydrophobic Structures of Plant Surfaces

Plant waxes are sometimes visible as a white or bluish coloration of leaves and fruits, such as grapes and plums. These colorations are induced by reflection of part of the visible light spectrum by a dense coverage of three-dimensional wax structures. The fan palm *Copernicia cerifera*, the natural source of carnauba wax, has massive crusts of epicuticular wax, weighing several mg/cm^2. Carnauba wax is commercially used, e.g., for car and furniture polishes, medical products, and candy. Even when there is not a bluish coloration visible, three-dimensional waxes can be present in lower amounts, or the waxes form thin films. In plants, three-dimensional waxes are responsible for several surface functions, such as reduction of wettability and decrease of energy uptake from the environment. Waxes are an integrative part of the plant cuticle, which covers the primary tissue of all aboveground parts of lower and higher land-living plants. Waxes occur as fillers of the basic cutin network (intracuticular), but are also on top of the cuticle (epicuticular). The epicuticular waxes occur in different morphologies, which all are crystalline, and it is well known that the wax morphologies originate by self-assembly. However, waxes of different plants, and also waxes of different parts of a plant, can vary in their morphology and chemical composition. In general, plant waxes are mixtures of long-chain hydrocarbons and their derivates, and in some species they also contain cyclic compounds. Because of the strong correlation between the wax crystal morphology and their chemical composition, some waxes, such as the nonacosanol tubules of the lotus leaves, have been named after their main wax constitution. The most common wax morphologies, their chemical composition, their self-assembly, and functions are introduced here.

Chemistry and Morphology of Plant Waxes

The term *wax* is used for a variety of natural or artificial commercial products that contain fatty materials of various kinds. Well-known examples are beeswax, paraffin, and carnauba wax from wax palms (*Copernicia cerifera*) (*Arecaceae*). Plant waxes are mixtures of aliphatic hydrocarbons and their derivatives with carbon chain lengths between 20 and 40, and in the case of esters (two connected chains) about 60 atoms. Several reviews have addressed the chemical composition of plant waxes [41.11, 22, 23]. The chemical composition of plant waxes is highly variable amongst plant species, the organs of one species (e.g., different leaves), and during organ ontogeny [41.24]. The main component classes are primary and secondary alcohols, ketones, fatty acids, and aldehydes. Alkanes are very common in plant waxes, but usually occur in low concentrations. Other compounds are more rarely found in plant waxes, but in those waxes where they occur, they may be the dominating compound. The most common wax compounds and their typical chain length are listed in Table 41.1. Examples of frequently existing waxes and their major compounds are presented in Table 41.2. For some of those waxes, it has been shown that their dominating compounds crystallize in the same morphology as the complete wax mixture. Examples are the primary alcohols and the β-diketone waxes found on different parts of wheat plants. However, an increasing number of publications report the discovery of new wax components, and a long list of rare and uncommon ingredients, such as methyl-branched aliphatics, have been reported [41.25]. Environmental factors, such as temperature or light intensity, may change the amount of waxes rather than their chemical composition [41.26–28].

Many plant waxes do not match the chemical definition of true waxes. For example, triterpenoids are cyclic hydrocarbons, which occur in high concentrations in the epicuticular coatings of grapes (*Vitis vinifera*) [41.26]. Other plant waxes contain polymeric components such

Table 41.1 The commonest chemical compounds in plant waxes and their spectrum of chain length. Further examples are given in Table 41.2

Aliphatic compounds **Frequently existing in waxes, but mostly as minor compounds**		**Chain length**
Alkanes	$CH_3–(CH_2)_n–CH_3$	Odd $C_{19}–C_{37}$
Primary alcohols*	$CH_3–(CH_2)_n–CH_2–OH$	Even $C_{12}–C_{36}$
Esters	$CH_3–(CH_2)_n–CO–O–(CH_2)_m–CH_3$	Even $C_{30}–C_{60}$
Fatty acids	$CH_3–(CH_2)_n–COOH$	Even $C_{12}–C_{36}$
Aldehydes	$CH_3–(CH_2)_n–CHO$	Even $C_{14}–C_{34}$
Rarely existing in waxes, but if present, than major wax compounds		
Ketones, e.g. palmitones	$CH_3–(CH_2)_n–CO–(CH_2)_m–CH_3$	Odd $C_{25}–C_{33}$
β-Diketones	$CH_3–(CH_2)_n–CO–CH_2–CO–(CH_2)_m–CH_3$	Odd $C_{27}–C_{35}$
Secondary alcohols, e.g. nonacosan-10-ol	$CH_3–(CH_2)_n–CH_2OH–(CH_2)_m–CH_3$	Odd $C_{21}–C_{33}$
Cyclic compounds		
Flavonoids	e.g. Quercetin	
Triterpene	e.g. β-Amyrin	

* Primary alcohols are common minor constitutions in waxes, but can occur as major compounds in the wax, e.g. of grasses, eucalypts, clover and other legumes, etc. [41.11]

Table 41.2 Common wax types in plant species and their major chemical compounds. With the exception of the fruit surface of *Benincasa hispida*, data represent the waxes on the leaves of the species. All references for the chemical data are listed in *Ensikat* et al. [41.33], and examples of the wax types listed here are shown in Fig. 41.4

Wax type	**Species**	**Dominating chemical compound(s)**
Films	*Hedera helix*	Primary alcohols, aldehydes
Films	*Magnolia grandiflora*	Fatty acids $C_{24}–C_{30}$, primary alcohols $C_{24}–C_{28}$
Films	*Prunus laurocerasus*	Alkanes C_{29}, C_{31}
Crust	*Crassula ovata*	Aldehydes C_{30}, C_{32}, alkanes C_{31}
Diketone tubules	*Eucalyptus globulus*	β-diketones C_{33}
Diketone tubules	*Leymus arenarius*	β-diketone C_{31}, hydroxy-β-diketone C_{31}
Nonacosanol tubules	*Ginkgo biloba*	Secondary alcohols C_{29}
Nonacosanol tubules	*Nelumbo nucifera*	Secondary alkanediols C_{29}
Nonacosanol tubules	*Thalictrum flavum glaucum*	Secondary alcohols C_{29}
Nonacosanol tubules	*Tropaeolum majus*	Secondary alcohols C_{29}
Nonacosanol tubules	*Tulipa gesneriana*	Secondary alcohols C_{29}
Platelets	*Convallaria majalis*	Primary alcohols C_{26}, C_{28}, aldehydes
Platelets	*Euphorbia myrsinites*	Primary alcohols C_{26}, aldehydes
Platelets	*Galanthus nivalis*	Primary alcohols C_{26}
Platelets	*Iris germanica*	Primary alcohols C_{26}
Platelets	*Triticum aestivum*	Primary alcohols C_{28}
Transversaly ridged rodlets	*Aristolochia tomentosa*	Ketones
Transversaly ridged rodlets	*Gypsophila acutifolia*	Alkanes C_{31}
Transversaly ridged rodlets	*Liriodendron chinense*	Ketones
Longitudinal ridged rodlets	*Benincasa hispida*	Triterpenol acetates

as polymerized aldehydes which are only slightly soluble in chloroform [41.29, 30]. It should be noted that nearly all the existing data on the chemical composition of plant waxes is based on solvent-extracted waxes. These are mixtures of epicuticular and intracuticular waxes, which may be chemically different, as shown

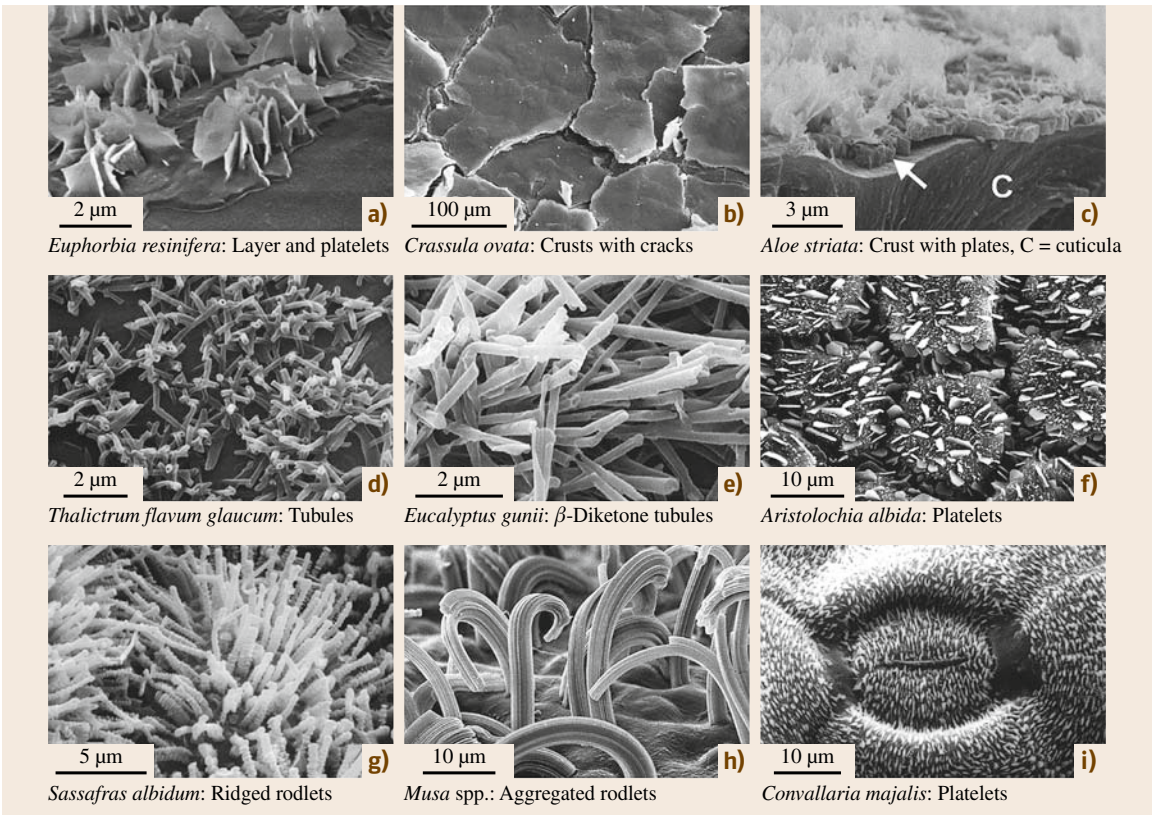

Fig. 41.4a–i SEM micrographs of epicuticular waxes. **(a)** Waxes on a leaf of *Euphorbia resinifera* have been partially removed to show the composite structure of the basal wax layer with three-dimensional wax platelets on it. **(b)** A wax crust with fissures on a leaf of *Crassula ovata*. A cross-section through the periclinal wall of *Aloe striata*. **(c)** The cuticle (indicated by C) and a wax layer (indicated by an *arrow*) with wax platelets on top. **(d)** Nonacosanol tubules on *Thalictrum flavum glaucum* leaves and **(e)** β-diketone wax tubules on *Eucalyptus gunnii* leaves. **(f)** Wax platelets on *Aristolochia albida* leaf and **(g)** transversely ridged rodlets on a leaf of *Sassafras albidum*. In **(h)** longitudinally aggregated wax threads form large aggregated rodlets on the lower side of the leaves of *Musa* spp. In *Convallaria majalis* leaves, shown in **(i)**, wax platelets are arranged in a pattern similar to magnetic field lines around the stomata. Thin wax films are not visible under SEM, but are present below and between the three-dimensional waxes shown here

for the waxes of *Prunus laurocerasus* by *Jetter* and *Schäffer* [41.24] and by *Wen* et al. [41.31] for *Taxus baccata*. The development of more selective methods of wax sampling allows selective removal of the epicuticular waxes and their analysis separately from the intracuticular wax fractions [41.24, 32].

Epicuticular wax structures usually occur in the size range from 0.2 to 100 µm; thus, the appropriate microscopic techniques for investigation of their morphology are SEM and low-pressure or environmental SEM. Several SEM investigations showed that most of the epicuticular waxes form three-dimensional structures, with great variations of their morphologies. Comprehensive overviews of the terminology and micromorphology of epicuticular waxes are given by *Barthlott* et al. [41.34] and *Jeffree* [41.11]. The classification of *Barthlott* et al. [41.34] includes 23 different wax types. It is based on chemical and morphological features and also considers orientation of single crystals on the surface and the orientation of the waxes to each other (pattern formation). In this classification, the wax morphologies include thin films and several three-dimensional structures such as crusts, platelets, filaments, rods, and tubules which have a hollow center. Morphological subtypes are, for example, entire and nonentire wax platelets. A further subclassification is

based on the arrangement of the crystals, e.g., whether they are randomly distributed, in clusters, in parallel orientation, or in specific arrangements around stomata, as in the *Convallaria* type. *Jeffree* [41.11] distinguishes six main morphological wax types, but suggests many more subtypes, based on chemical differences, found, e.g., for wax tubules. The most common wax morphologies are introduced in the following part and in Table 41.2.

That the three-dimensional wax crystals appear together with an underlying wax film shown in Fig. 41.4a, for the waxes of *Euphorbia resinifera* and has been reported for several species [41.34–38]. Wax films are often incorrectly referred to as an *amorphous* layer, more of a morphological description than a crystallographic one [41.33]. On several plant surfaces the wax film is limited to a few molecular layers which are hardly visible in the SEM. However, by mechanical isolation of the epicuticular waxes, e.g., freezing in glycerol, the waxes can be removed from the cuticle, and transferred onto a smooth artificial substrate for microscopic investigations [41.32]. By this method, the edges of the wax film can be detected, and the film thicknesses can be determined. Wax film formation has been investigated on a living plant surface by atomic force microscopy (AFM) [41.37]. Such investigations showed that wax films are composed of several monomolecular layers, with thicknesses up to several hundred nanometers. In the following, these relatively thin wax films ($< 0.5\,\mu m$) are called two-dimensional (2-D) waxes, and the thicker wax layers ($0.5–1\,\mu m$) and wax crusts ($> 1\,\mu m$) are called three-dimensional (3-D) waxes. Wax crusts are often found in succulent plants, as on the leaves of *Crassula ovata*, shown in Fig. 41.4b. In some species, three-dimensional waxes occur on a wax layer or wax film. Such a multilayered assembly of waxes is detectable by a cross-section through the epidermis, as shown in Fig. 41.4c for *Aloe striata*.

Three-dimensional waxes occur in different morphologies. The most common ones are tubules, platelets, rodlets, and longitudinally aggregated rodlets, as shown in Fig. 41.4d–i and introduced below. Wax tubules are hollow structures, which can be distinguished chemically as well as morphologically. The first type, called nonacosanol tubules, contains high amounts of asymmetrical secondary alcohols, predominantly nonacosan-10-ol and its homologs and to a certain degree also asymmetrical diols [41.39, 40]. These tubules can be found on most conifers, on lotus leaves, and in nearly all members of the *Papaveraceae* and *Ranunculaceae*, as shown on *Thalictrum flavum glaucum* in Fig. 41.4d [41.41]. Nonacosanol tubules are usually $0.3–1.1\,\mu m$ long and $0.1–0.2\,\mu m$ wide. The second type of tubules contains high amounts of β-diketones, such as hentriacontan-14,16-dione [41.42]. This particular kind of wax tubule is characteristic of several species of *Poaceae* but also occurs in various other groups [41.41]. Figure 41.4e shows that the β-diketone tubules are two to five times longer than the nonacosanol tubules shown in Fig. 41.4d. Their length ranges from 2 to $5\,\mu m$, and diameters vary between 0.2 and $0.3\,\mu m$. Platelets, as shown in Fig. 41.4f, are the most common wax structures, found in all major groups of plants. Following the terminology of *Barthlott* et al. [41.34], waxes are termed platelets when flat crystals are connected with their narrow side to the surface. Platelets can be further differentiated by their outline into, e.g., entire or undulated ones. In contrast, plates are polygonal crystalloids with distinct edges and are attached to the surface at varying angles. Platelets vary considerably in shape, chemical composition, and spatial pattern. For platelets, only limited information about the connection between morphology and chemical composition is available. In some species, wax platelets are dominated by high amounts of a single chemical compound, which can be primary alcohols, alkanes, aldehydes, esters, secondary alcohols or flavonoids [41.11]. The morphology of three-dimensional wax structures is not necessarily determined by the dominating chemical compound or compound class. One example of wax crystals determined by a minor component of a complex mixture are the transversely ridged rodlets, shown in Fig. 41.4g, which contain high amounts of hentriacontan-16-one (palmitone) [41.43]. Wax rodlets are massive sculptures which are irregular, polygonal, triangular or circular in cross-section. They have a distinct longitudinal axis, with a length-to-width ratio usually not exceeding 50 : 1. In addition, rodlets may have variable diameter along the length of their axis. More complex structures are the longitudinally ridged rodlets, such as those found on banana leaves (*Musa* species), shown in Fig. 41.4h. These waxes consist exclusively of aliphatic compounds, with high amounts of wax esters and less of hydrocarbons, aldehydes, primary alcohols, and fatty acids. The origin of these wax aggregates is still not clear, and so far all attempts to recrystallize these wax types have failed. As a consequence, it is assumed that their origin is connected to structural properties of the underlying plant cuticle. A very complex wax crystal morphology is known from *Brassica oleracea*, in which several cultivars form several different wax types, and where several different

wax morphologies can occur on the same cell surface [41.26]. It is still an unanswered question, why do different three-dimensional wax morphologies coexist even on the surface of a single cell, and whether these different morphologies are built up by phase separation of different compounds or by the same compound.

The last example shown in Fig. 41.4i represents plant surfaces on which waxes are arranged in a specific pattern. Examples are parallel rows of longitudinally aligned platelets, which always exceed one cell (e.g., in *Convallaria majalis*), or rosettes, in which the arrangements of platelets is more or less in radially assembled clusters. In particular, the parallel orientation of platelets on the leaves of several plant species leads to the question of how the orientation is controlled by the plant. It is assumed that the cutin network functions as a template for the growth of the three-dimensional wax crystals, but there is still a lack of information about the molecular structure of the cuticle, so this question cannot be answered yet.

Certain surface wax morphologies and their orientation patterns are characteristic for certain groups of plants; thus, patterns and the morphology of plant waxes have been used in plant systematics. *Barthlott* et al. [41.41] provide an overview of the existence of the most important wax types in plants, based on SEM analysis of at least 13 000 species, representing all major groups of vascular plants.

Crystallinity of Plant Waxes

All aliphatic plant surface waxes have crystalline order. The classical definition of crystals implies a periodic structure in three dimensions, but with the increasing importance of liquid crystals and the detection of quasicrystals it has become necessary to extend the definition, so that certain less periodic and helical structures, as found for some waxes, are included [41.44].

The crystal structure of the epicuticular waxes can be examined by electron diffraction (ED), nuclear mass resonance (NMR) spectroscopy, and x-ray powder diffraction (XRD). Electron diffraction with the transmission electron microscope provides structural information for single wax crystals of less than 1 μm size, as shown in Fig. 41.5a,b for a single wax platelet. However, even with a low-intensity imaging system, the crystal structure is rapidly destroyed by the electron beam intensity. Therefore, XRD is useful to determine the crystal symmetry, and it provides information about different types of disorder. Very thin mono- or bimolecular layers of waxes, as shown in Fig. 41.5c,d, are of course not periodic in three dimensions, but form, in regard to the entire molecules, two-dimensional (2-D) crystals. Besides the planar wax structures such as films and platelets, many natural plant waxes develop irregular three-dimensional morphologies, or structures such as threads and tubules with large extension in one direction. These morphologically different waxes were found to occur in three different crystal structures. The majority of waxes exhibit an orthorhombic structure, which is the most common for pure aliphatic compounds. Tubules containing mainly secondary alcohols show diffraction reflections of a triclinic phase, with relatively large disorder, and β-diketone tubules show hexagonal structure [41.33].

Self-Assembly of Plant Waxes

That different wax morphologies on plant surfaces originate by self-assembly of the wax molecules has been shown by the recrystallization of waxes isolated from plant surfaces [41.36, 37, 40, 45–47]. In these studies, most waxes recrystallized in their original morphology, as found before on the plant surfaces.

Self-assembly processes resulting in nano- and microstructures are found in nature as well as in engineering. They are the basis for highly efficient ways

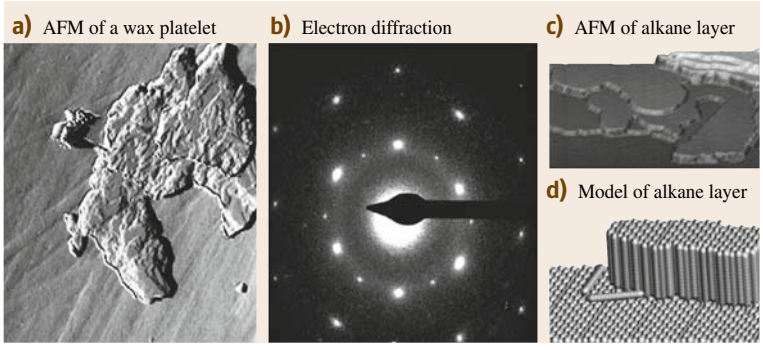

Fig. 41.5a–d The layered and crystalline structure of alkane waxes is demonstrated by an AFM map of a single wax platelet **(a)** and the corresponding electron diffraction pattern **(b)**. In **(a)** the steps visible on the crystal surface are caused by perpendicular orientation of the molecules. Such steps can be monomolecular, e.g., for alkanes, or in some waxes bilayers are formed by polar molecules such as primary alcohols. The AFM map of recrystallized alkanes **(c)** and the model shown in **(d)** demonstrate the layered orthorhombic wax structure

of structuring surfaces reaching down to the molecular level. Self-assembly is a general process of structuring in which atoms, molecules, particles or other building units interact and self-organize to form well-defined structures [41.48]. The processes of self-assembly in molecular systems are determined by five characteristics: the components, interactions, reversibility, environment, and mass transport with agitation [41.49]. The most important driving forces are weak and noncovalent intermolecular interactions, such as van der Waals and Coulomb interactions, hydrophobic interactions, and hydrogen bonds. During self-assembly, their interactions start from a less-ordered state, e.g., dissolved waxes in a solution, to a final more-ordered state, a crystal [41.50, 51]. Environmental factors such as temperature, solvent, and substrate might influence the self-assembly process, and in the case of waxes, their morphology.

The most suitable microscopy technique for studying the self-assembly process of waxes under environmental conditions is AFM because it combines sufficient resolving power to image nanostructures with the ability to work at standard temperature and pressure (STP) with living plant material. Self-assembly of waxes has been studied directly on plant surfaces, but also by recrystallization of waxes and single wax compounds on artificial surfaces. However, AFM is not suitable for all plant surfaces. Within a leaf surface large structures such as hairs with dimensions of several tens of micrometers can emerge out of the epidermis and pose a barrier against the surface scanning probe. Additionally, high-aspect-ratio structures caused by cell surface structures might cause artifacts in the resulting images. Species with smooth or slightly convex cell surface sculptures are most appropriate for AFM investigations. The process of wax regeneration occurs over several hours; thus the loss of water from inside the plant has to be minimized to reduce specimen drift by material shrinkage during investigation. This precondition limits the range of specimens for AFMs with a small specimen chamber, because the sizes and shapes of the leaves must allow them to be mounted in the AFM without cutting them. An experimental setup where the complete plant is placed close to the AFM and a leaf is fixed on the AFM specimen holder is shown in Fig. 41.6. In this, the leaf was fixed at its lower side to the specimen holder with a drop of a two-compound glue, and waxes on the upper leaf side were removed by embedding them into a drop of water-based glue. After hardening, the glue and the embedded waxes can be removed from the leaf surface and the process of wax regeneration can be studied. Temperature increase in long-term investigations, caused by the laser beam on top of the cantilever, induces expansion of the water-containing leaf, and therewith a drift of the specimen. To minimize this, reflective cantilevers must be used, and the laser beam intensity should be reduced by integrating an attenuation filter above the cantilever [41.37]. However, the waxes themselves are fragile; thus appropriate scan conditions at scan sizes of 3–20 μm are tapping mode and scan rates of 0.7–2 Hz, encompassing 256 lines per image and a set point near the upper limit to minimize the interaction between tip and sample. Figure 41.7 shows the regeneration of a wax film on a leaf of snowdrop (*Galanthus nivalis*) by formation of a multilayered wax film and the growth of three-dimensional wax platelets. This and further investigation showed that the growth of the three-dimensional wax crystals occurs by apical accumulation of new wax molecules on only one side of the crystal. The regeneration of the wax film results in a multilayered crystalline coverage on the plant cuticle. The time needed to regenerate removed waxes shows large variations in different species and some species do not even regenerate removed waxes. In these plants, wax synthesis seems to be inactive when leaves are mature [41.52].

Self-assembly of plant waxes can alternatively be studied by recrystallization of the waxes on smooth

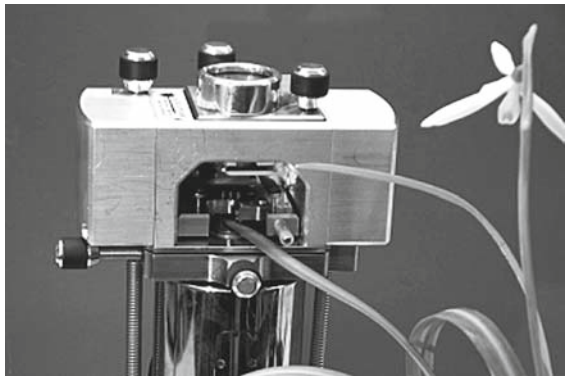

Fig. 41.6 AFM experimental setup for long-term investigations of wax crystallization on a living plant surface. The tip of the leaf of *Galanthus nivalis* has been fixed onto the specimen holder with a drop of two-compound glue. Existing waxes have been removed and the rebuilding (self-healing) of the wax can be studied over several hours. Appropriate scan conditions for living plant surfaces are given in the text and the method of wax removal is described in detail by *Koch* et al. [41.37]

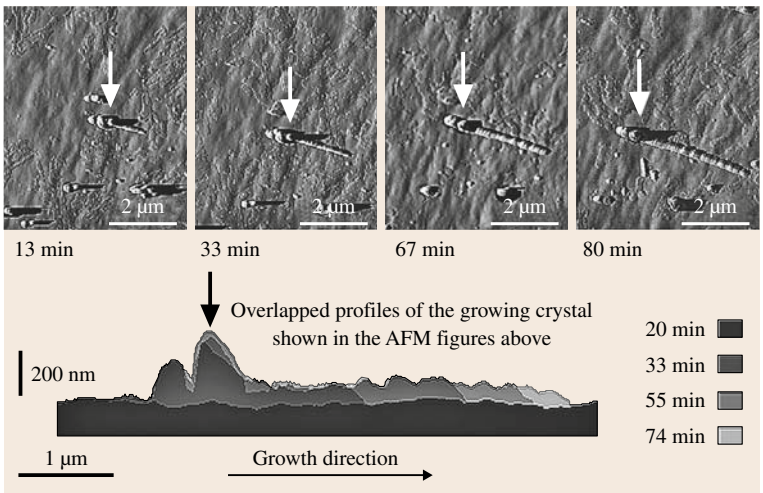

Fig. 41.7 AFM maps and a series of profile lines, taken from repeated scans during crystal growth on a leaf of snow belt (*Galanthus nivalis*). The first AFM map represents wax regeneration within 13 min; the last map was taken 80 min after wax removal. The *white arrows* mark the same position of the crystal as the *black arrow* marks in the profile figure. In the lower figure, the outlines of the growing crystal have been overlapped to demonstrate that the extension is occurring at the distal end of the growing crystal and that at this time the growth in height is limited to a few nanometers. Outlines were taken from four AFM scans, 20, 33, 55, and 74 min after the wax regeneration process started. The experimental setup is shown in Fig. 41.6

artificial substrates. Based on those studies, the formation of wax tubules and platelets has been described in detail. Wax platelets, characteristic of wheat leaves (*Triticum aestivum*), are constructed from the primary alcohol octacosan-1-ol [41.46]. Crystallization of the wax mixture isolated from the leaves and of pure octacosan-1-ol on different artificial substrates showed substrate-dependent growth. On a nonpolar, crystalline substrate (highly ordered pyrolytic graphite, HOPG) platelets grow with a vertical orientation to the substrates, whereas on a polar surface, such as mica, crystals grow horizontally to the substrate surface. On amorphous polar glass only amorphous wax layers grow. This substrate dependence demonstrates epitaxial control of crystal growth depending on the orientation and order of the first layers of molecules adhering on the substrate surface. Octacosan-1-ol forms ordered bilayer structures on the substrate. In these, the first layers of molecules lie flat on nonpolar substrates, but stand upright (perpendicular) on crystalline polar surfaces. The grown platelet morphology results from an anisotropic crystal growth, caused by faster parallel assembly of the molecules at the length side of already existing molecules than at the ends of the molecules [41.53]. AFM micrographs in Fig. 41.8 and schematics of the molecule orientation demonstrate the differences of growth on polar and nonpolar substrates for octacosan-1-ol molecules. In both cases, flat crystals with different orientation grow. Crystals grown horizontal to the substrate surface are called plates (Fig. 41.4a,b), whereas those grown perpendicular to the substrate surface are termed platelets (Fig. 41.4c,d). The substrates on which crystals grow influence the crystal morphology and their orientation. This fact can be used to create different kinds of nano- and micropatterns on technical surfaces [41.46, 47, 54, 55]. In summary, substrates can have a direct influence on the self-assembly processes of wax crystals, and can function as a template on the molecular level. In such a case, the substrate organizes the

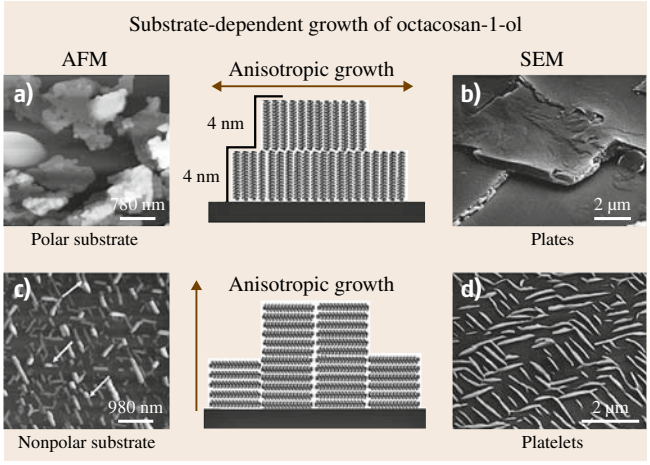

Fig. 41.8a–d AFM maps and schematics of the molecular orientation demonstrate the differences between growth on polar and nonpolar substrates for octacosan-1-ol molecules. AFM figures **(a,c)** show growing crystals, whereas the SEM figures **(b,d)** show the final crystal morphology. On both substrates flat crystals with different orientations were grown. Crystals grown horizontal to the substrate surface **(a,b)**, whereas those grown perpendicular to the substrate surface **(c,d)** are termed platelets. The principle of anisotropic crystal growth is shown schematically for both preferred growth directions and is described in the text

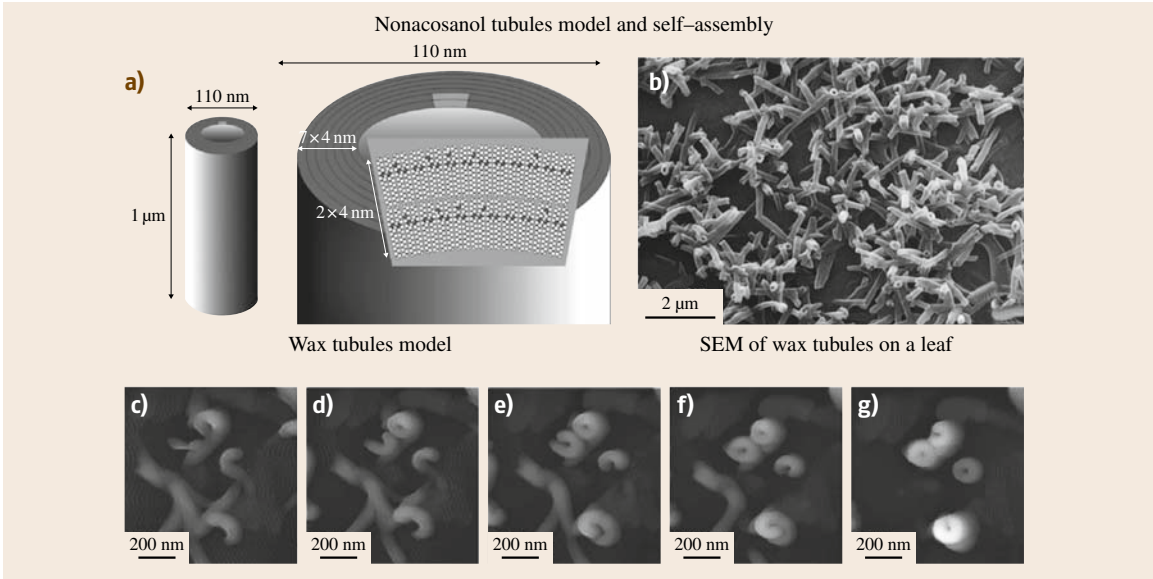

Fig. 41.9a–g A model and SEM micrograph of the molecular order of nonacosanol tubules, and AFM analysis of their self-assembly. Based on SEM characterization, chemical analysis, single-compound crystallization, and crystallographic data, a model of nonacosan-10-ol tubules has been developed **(a)**. Original nonacosan-10-ol tubules are shown in the SEM micrograph **(b)** for *Thalictrum flavum glaucum* leaves. Consecutive AFM figures of tubule formation (nonacosan-10-ol wax from *Tropaeolum majus*) were made after applying a wax solution on HOPG. After 65 min **(c)** the waxes mainly formed curved rodlets, which were arranged horizontally to the substrate. The same area of the HOPG substrate shows that waxes start to form **(d–f)** circles and, after 223 min **(g)**, the initially observed rodlets were dissolved and short tubules were formed

assembly of the molecules in a specific spatial arrangement [41.56,57]. Such a template effect was reported for wax platelets formed by primary alcohols [41.46]. On HOPG substrate, the spatial pattern of the reassembled wax platelets strictly followed the hexagonal symmetry of the crystalline substrate. However, the cutin matrix of the cuticle, which acts as a substrate in plant surfaces, is supposed to be amorphous, and epitaxial growth on an amorphous substrate seems unusual.

Wax crystals which are composed of more than one compound are, for example, the transversely ridged rodlets. These waxes can be recrystallized from the total wax mixture, but not from individual compounds such as alkanes or palmitones. For these waxes, it is assumed that their morphology is also formed by a self-assembly-based crystallization process, but the presence of minor amounts of other compounds is required as an additive for crystal growth [41.43].

The origin of wax tubules, shown schematically in Fig. 41.9a and in SEM micrographs in Fig. 41.9b, has been debated for a long time. Several observations, such as spiral lines on the surfaces of some nonacosanol tubules [41.45], led to the assumption that tubules arise from a twisting or folding of a platelet-like precursor form. Recrystallization experiments with nonacosanol waxes showed that these tubules grow perpendicular to the substrate surface when recrystallized on HOPG. This vertical orientation of the tubules allows detailed study of the growth process by AFM and showed that the building of nonacosan-10-ol tubules from lotus (*Nelumbo nucifera*) and nasturtium (*Tropaeolum majus*) leaves is based on a continuous growth of a small circular precursor structure by supplementation of the wax on top of it [41.47]. The micrographs in Fig. 41.9c–g show consecutive AFM images of growing tubules, made during the tubule formation process. The terminal ends of growing tubules are asymmetric in height. This asymmetry seems to be caused by an accumulation of new wax molecules at edges found at the terminal end of the tubules and indicates a helical growth mechanism for the tubules. The pure nonacosan-10-ol alcohol, the dominating compound of wax tubules, can crystallize in different forms [41.36, 40, 45]. *Jetter* and *Riederer* [41.40] showed that a range

of alkanediols, present in the waxes of many secondary alcohol tube-forming species, also have tube-forming capability.

Chemical analysis of the leaf waxes of lotus and nasturtium *(Tropaeolum majus)* showed that waxes of both species are composed of a mixture of aliphatic compounds, with nonacosan-10-ol (a secondary alcohol) and nonacosandiols (an C_{29} alkane with two alcohol groups) as their main components [41.47]. These compounds have been separated from the rest of the wax compounds and used for recrystallization experiments. It could be shown with mixtures of nonacosan-10-ol and nonacosandiols components that a minimum amount of 2% of nonacosandiols supports tubule formation [41.58].

Analysis of wax chemistry, crystalline order, and their self-assembly has led to better understanding of the molecular architecture of three-dimensional waxes. Based on these data, a model of nonacosan-10-ol tubule structure has been developed, as shown in Fig. 41.9a. Here it is assumed that the lateral oxygen atoms at the side of the straight molecules hinder the formation of the normal, densely packed, orthorhombic structure and require additional space, causing local disorder between the molecules and thus spiral growth, leading to the tubule form.

41.1.3 From Single Cell to Multicellular Surface Structuring

Millions of years of plant evolution have resulted in a variety of plant functional surface structures. Optimized structures can be found in different environments, for example, the water-repellent and self-cleaning leaves of lotus (*Nelumbo nucifera*), which are specialized surfaces for pathogen defense in humid environments. In plants, surface structuring arises at different hierarchical levels. The epidermal cells create sculpturing of the surfaces on the microscale, but on a smaller scale the surfaces of individual cells are structured as well. In the following, the origin of surface sculpturing in plants is introduced, and the basic terminology for their description is given. The first part gives an overview about plant surface structures which are formed by a single cell, including the shape and sculpture of the cell and the structures of the cell surface. The second part includes multicellular sculptures. For a broader understanding, we try to avoid the use of many specialist terms here and use more common names, and scientific designations are placed in brackets.

Cellular Surface Structures in Plants

The Outlines of Cells. The description of plant micro- and nanostructures requires the use of some basic uniform terms, for example, to describe the outline of a single epidermis cell. Several variations are known and introduced in detail by *Barthlott* and *Ehler* [41.59], *Barthlott* [41.60], and *Koch* et al. [41.1–4]. In the following, a brief introduction is given.

The boundary walls between two adjacent epidermal cells are called anticlinal walls, whereas the outer wall forming the cell surface is called the periclinal wall. The primary sculpture of a single cell encompasses the outline, including the shape and relief of the anticlines and curvature of the outer periclinal wall. There are two basic forms of cells, the tetragonal and polygonal form, both of which can have a uniform length of their sides or be elongated. Additionally, the course of the anticlinal walls can be straight or un-

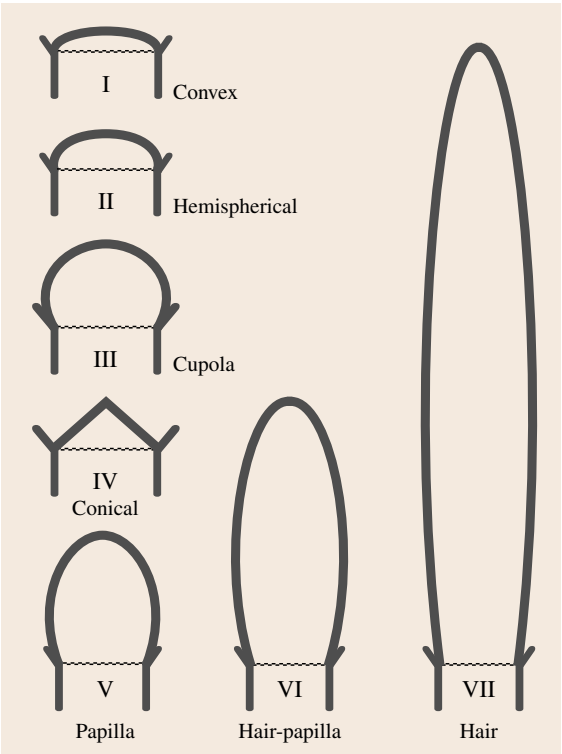

Fig. 41.10 Schematics and terminology of the different convex cell outlines and their aspect ratios (β = width/height): (I) convex ($\beta \geq 3/1$), (II) hemispherical ($\beta \approx 2/1$), (III) cupola ($\beta < 3/2$), (IV) conical ($\beta > 3/2$), (V) papilla ($\beta < 3/2$ and $> 1/2$), (VI) hair-papilla ($\beta < 1/3$ and $> 1/6$), and (VII) hair ($\beta < 1/7$)

even. It is assumed that the outline of anticlines has an influence on the mechanical stability of the epidermis tissue, but experimental evidence for this hypothesis is not available. The cell sculptures or curvature of the outer epidermis wall (periclinal wall) can be tabular (flat), convex (arced to the outside) or concave (arced to the inside), and has a great influence on the surface roughness on the micrometer scale. Additionally, only the central area of a cell can form a convex outgrowth and form a papilla or hair-like structure. The convex cell type is the most common cell type of epidermal surfaces, often found on flower-leaves, stems, and leaves [41.61]. These cell morphologies originate by expansion of the outer side (periclinal wall) of the epidermis cells. They can be divided into several subtypes, depending on the outline of the epidermis cells and their aspect ratio (width to height), which determines their designation. In Fig. 41.10 a schematic of different convex cell outlines and their designations is given. The terminology is based on the cell outline and aspect ratios (β = width/height) of the cells and includes: convex ($\beta \geq 3/1$), hemispherical ($\beta \approx 2/1$), cupola ($\beta < 3/2$),

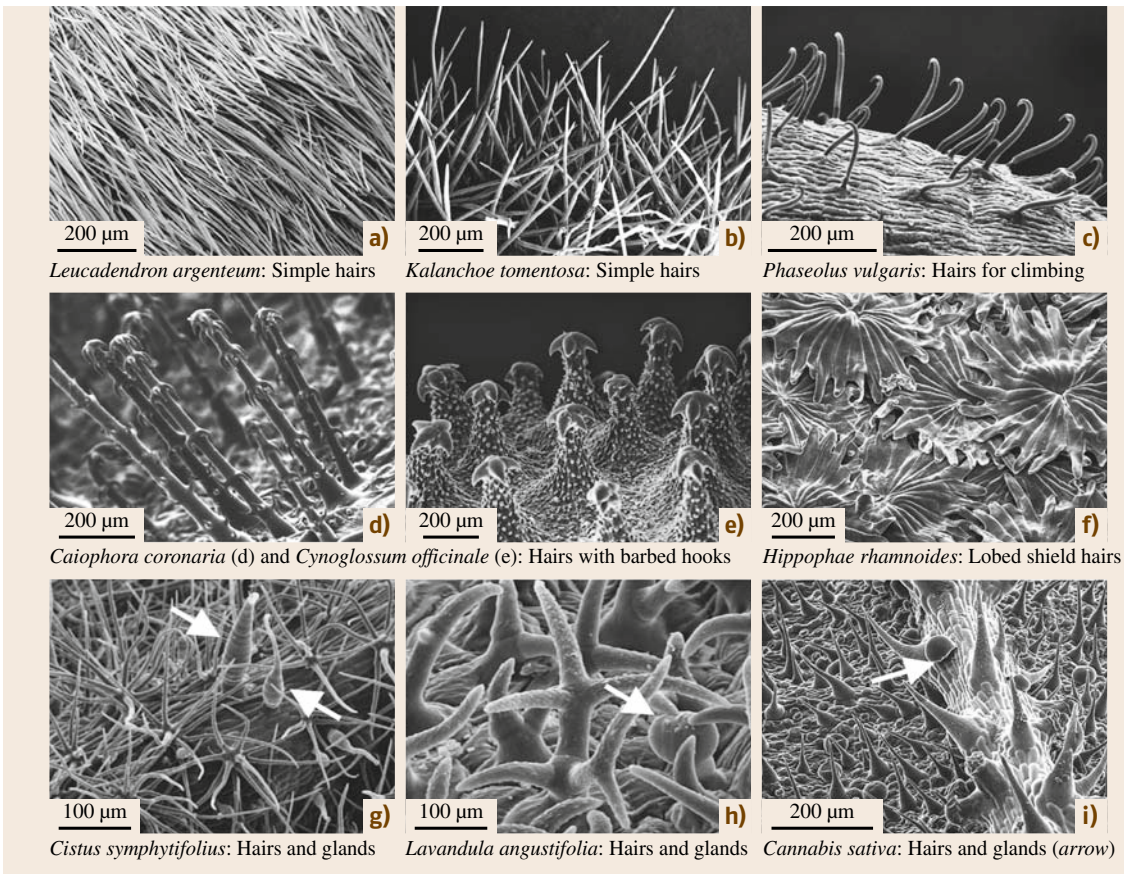

Leucadendron argenteum: Simple hairs — *Kalanchoe tomentosa*: Simple hairs — *Phaseolus vulgaris*: Hairs for climbing

Caiophora coronaria (d) and *Cynoglossum officinale* (e): Hairs with barbed hooks — *Hippophae rhamnoides*: Lobed shield hairs

Cistus symphytifolius: Hairs and glands — *Lavandula angustifolia*: Hairs and glands — *Cannabis sativa*: Hairs and glands (*arrow*)

Fig. 41.11a–i SEM micrographs of hairs and glands on plant surfaces. A dense layer of straight, unbranched hairs, almost orientated parallel to the leaf surface on *Leucadendron argenteum* leaf **(a)**. The unbranched hairs of *Kalanchoe tomentosa* shown in **(b)** are orientated upright. The shoot surface of the climbing bean plant *Phaseolus vulgaris* with terminal hooks is shown in **(c)**. Single hairs on a leaf of *Caiophora coronaria* **(d)** and those on the seed surface of *Cynoglossum officinale* **(e)** are characterized by terminal and lateral barbed hooks. The peltate hairs of *Hippophae rhamnoides* **(f)** form lobed shields. Simple branched star-like hairs and two morphologically different glands (*arrows*) on the leaf of *Cistus symphytifolius* are shown in **(g)**. Multiple ramified hairs and short-stalked glands (*arrow*) on a leaf of *Lavandula angustifolia* are shown in **(h)**. In **(i)** an exposed leaf vessel with hair-papilla and unstalked glands (*arrow*) of *Cannabis sativa* is shown. **(a–h)** were obtained from upper (adaxial) leaf sides and **(i)** from the lower (abaxial) leaf side

conical ($\beta > 3/2$), papilla ($\beta < 3/2$ and $> 1/2$), hair-papilla ($\beta < 1/3$ and $> 1/6$), and hairs ($\beta < 1/7$). In these, hairs are built by the outgrowth of a single surface cell. Hairs are often named trichome (Greek: *trichoma*).

The leaf surfaces of *Leucadendron argenteum* and *Kalanchoe tomentosa*, shown in the SEM micrographs in Fig. 41.11, are two representative surfaces with hairs. Hairs can decrease, but also increase, the loss of water and influence the wettability of the surfaces [41.62]. The wide spectrum of functions of plant hairs has been reviewed by *Wagner* et al. [41.63], and more recently by *Martin* and *Glover* [41.61]. With respect to their functions, it is important to notice that hairs can be glandular or nonglandular (nonsecreting), dead or living, and hairs can also be built up by several cells (multicellular), which are introduced later. Unicellular trichomes can be found on the aerial surfaces of most flower-plants (angiosperms), some conifers (gymnosperms), and on some mosses (bryophytes) [41.63]. Many plants of dry habitats show a dense cover of dead, air-filled hairs to reflect visible light, which makes the surfaces appear white. Two examples are the South-African protea tree *Leucadendron argenteum* (Fig. 41.11a) and *Kalanchoe tomentosa* (Fig. 41.11b). The structures of hairs are often more complex; thus, the definition based on the aspect ratio fits well only for simple, undivided hairs. On kidney shoots (*Phaseolus vulgaris*), hairs form hooks to get better adhesion for climbing (Fig. 41.11c) and in *Caiophora coronaria* (Fig. 41.11d) and *Cynoglossum officinale* (Fig. 41.11e) the hairs have lateral barbed hooks. The hairs of *Hippophae rhamnoides* form lobed shields (Fig. 41.11f). Further trichomes are the simple or double-branched hairs and secretion glands on the leaves of *Cistus symphytifolius*, *Lavandula angustifolia*, and *Cannabis sativa* (Fig. 41.11g–i). These complex hair structures require a more differentiated description than the aspect ratio used for simple hairs [41.64, 65]. The sizes and morphologies of trichomes are often species specific, which makes some trichomes useful as morphological features in plant systematics [41.65].

A different surface structure is formed by concave cells. Cell shrinking induced by water loss from the cells might lead to concave cell morphology, thus concave cells are seldom found on water-containing epidermal cells, but occur often on dry seed surfaces (testa cells) [41.66]. They are characterized by complete or particular deflection of the outer epidermis wall. The concave cell type is characteristic for small, wind-dispersed seeds, as for *Aeginetia indica* and *Triphora trianthophora* (Fig. 41.12).

The Structures of Cell Surfaces. Surface structuring is also related to the fine structures of cell surfaces. In plants, four frequently found morphological modifications of the outermost epidermis cell layers are known. These modifications are shown schematically in Fig. 41.13. In the first case, shown in Fig. 41.13a, the surface structure is induced by concavities of the cell wall which lead to coves and folding of the surface. The second kind of structuring originates by subcuticular inserts of mineral crystals, such as silicon oxides (Fig. 41.13b). The third kind of surface structuring results from folding of the cuticle itself (Fig. 41.13c). Additionally, on many plants, waxes on top of the cuticle lead to surface structuring, as shown in Fig. 41.13d.

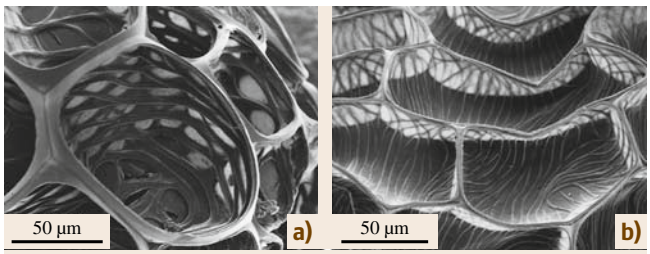

Collapsed cells of seed surfaces: *Aeginetia indica* (a) and *Triphora trianthophora* (b)

Fig. 41.12a,b SEM micrographs of two seed surfaces with concave cell sculpturing. Seeds of both species **(a)** *Aeginetia indica* and **(b)** *Triphora triantophora* are examples of lightweight constructions, optimized for seed dispersal by wind. The concave structure of the dead cells can be interpreted as due to shrinkage deformation during seed maturation and death. The bands which form an inner network in **(a)** and the surface pattern in **(b)** are build by cellulose

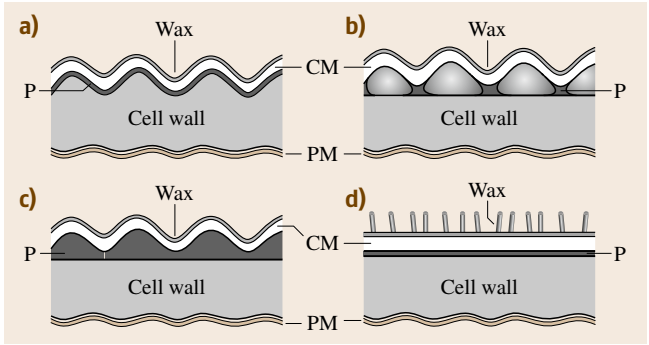

Fig. 41.13a–d Schematic cross-sections through plant epidermis cells showing different sources leading to microstructuring of cell surfaces. In **(a)** the surface profile is induced by coves of the underlying cell wall, in **(b)** by insertion of subcuticular minerals, in **(c)** by folding of the cuticle, and in **(d)** by waxes located on top of the cuticle (epicuticular wax). Wax = epicuticular waxes, CM = cuticular membrane, P = pectin, PM = plasma membrane (after [41.59])

Waxes and their structural diversity have already been introduced; thus in the following, cuticular folds and subcuticular inserts are introduced.

Cuticular patterns have been described for nearly all aboveground surfaces of plants, but are very frequently found in the leaves of flowers (petals), and on seed surfaces. They occur as folding or tubercular (verrucate) patterns, which originate due to the cuticle itself, by the expression of the bulk of the cell wall below, or by subcuticular deposits. The pattern of cuticular folds can be categorized according to the thickness (width) of the folds, distances between the folds, and by their orientation [41.59]. Additionally, the pattern of folding within a single cell can be different in the central (inner area) and anticlinal field (outer area) of a cell. Figure 41.14 shows different patterns of cuticle folding. On the leaves of *Schismatoglottis neoguinensis* (Fig. 41.14a,b) the folding is orderless and covers the central and anticlinal field of the cells. On the lower leaf side (adaxial) of *Alloca-*

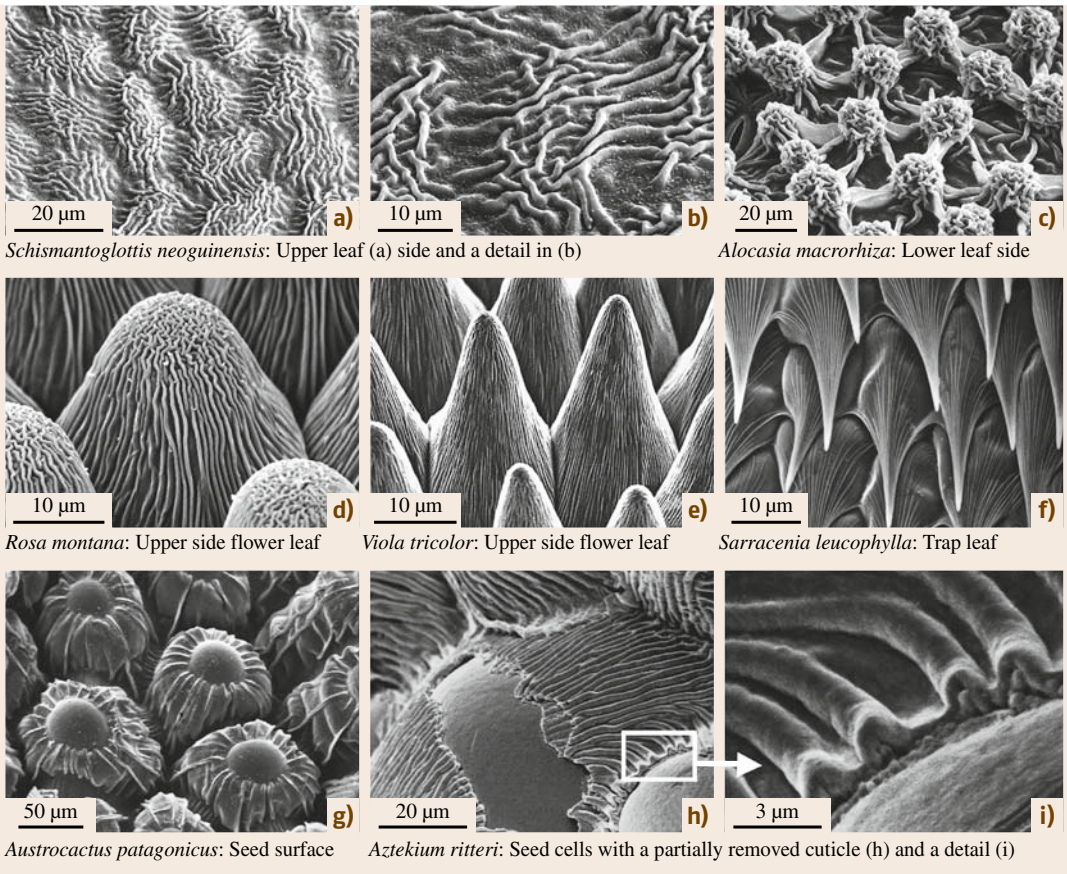

Fig. 41.14a–i SEM micrographs of cell surfaces with cuticular folding. In **(a,b)** the irregular cuticular folding on a leaf of *Schismatoglottis neoguinensis* is restricted to the central field of the cells. In **(c)** *Alocasia macrorhiza*, the cells are flat (tabular), with exposed node-like foldings in the central fields of the cells. The cells of a flower petal of *Rosa montana* with a rippled folded cuticle in the central field of the cells and parallel folding, running to the anticlinal walls of the cells, is shown in **(d)**. In **(e)** conical cells of the flower petals of *Viola tricolor* with parallel folding are shown. Cells of the inner side of a tube-like leaf of the carnivorous plant *Sarracenia leucophylla* are shown in **(f)**. These cells have a conical hair-papilla in the downward direction with parallel cuticle folding, with larger distances of the folds at the base and denser arrangement at the cell tip. In **(g–i)** seed surfaces are shown. In *Austrocactus patagonicus* **(g)** the central field of the cells is unstructured, whereas a rough folding exists in the anticlinal fields. In *Aztekium ritteri* **(h,i)** a part of the cuticle has been removed to show the cuticle folding

sia macrorhiza, shown in Fig. 41.14c, the cuticle forms node-like folding in the central part of each cell. The flower petals of *Rosa montana*, shown in Fig. 41.14d, have convex cells with a small central field with a rippled folded cuticle and parallel folds in the anticlinal field. The papilla cells of the flower petals of *Viola tricolor*, shown in Fig. 41.14e, have a parallel folding from the center to the anticlines of the cells. The cells inside the trap of the carnivorous plant *Sarracenia leucophylla*, shown in Fig. 41.14f, are hair-papillae, with a conical shape curved in a downward direction. On these, a parallel cuticle folding exists with larger distance at the base and a denser arrangement at the cell tip. The seed surface of *Austrocactus patagonicus*, shown in Fig. 41.14g, has cupolar-formed cells with unstructured central fields and broad parallel folds in the anticlinal fields. A high-magnification SEM micrograph of the seed surface of *Aztekium ritteri*, shown in Fig. 41.14h,i, shows a partially removed cuticle and demonstrates that the origin of surface folding is caused by the cuticle itself.

The functional aspects of cuticle folding are rarely investigated, but their frequent occurrence on flower petals has led to the assumption that cuticular folding forms a favorable structure for insect pollinators for walking on them. *Kevan* and *Lanet* [41.67] gave evidence that cuticular folding in flower petals is a tactile cue for bees to find the nectar source of the flowers. *Maheshwari* [41.68] reported that cuticular folding is a signal for the germination of fungi. Evidence for this hypothesis is based on in vitro investigations with structured biomimetic surfaces, microfabricated by electron-beam lithography [41.69].

Barthlott and *Ehler* [41.59] observed that cuticular folding and their characteristic pattern already exist in very young organs, and that only the amount of folding per area might increase during parthenogenesis of the organs. However, the formation and function of these complex structures are not yet completely understood.

Some microstructures on epidermis cells arise from subcuticular inserts of mineral crystals, as indicated in Fig. 41.13b. These subcuticular inserts can be solid crystals of silicon dioxide, as shown in Fig. 41.15 for the leaves of rice (*Oryza sativa*) and for tin plant or horse tail (*Equisetum*) plants. Calcium oxalate crystals are also frequently found in plants, and the presence of silicon or calcium can be verified simply by energy-dispersive x-ray (EDX) analysis, equipped in an SEM. Silicon (Si) is a bioactive element associated with beneficial effects on mechanical and physiological properties of plants. It is a common element found in plants and occurs as monosilic acid or in the polymerized form as phytoliths ($SiO_2 \cdot nH_2O$) [41.70]. In plants, Si tends to crystallize in the form of silica in cell walls, cell lumen, at intercellular spaces, and in the subcuticular layer [41.71]. Silica increases the resistance of plants to pathogenic fungi. This protective function seems to be based on a genetically controlled defense mechanism and cannot be interpreted as a function of increased mechanical stability [41.72].

Calcium oxalate crystals have been reported for more than 250 plant families of the gymnosperms and angiosperms [41.73]. Calcium oxalate crystals occur in five different morphological variations, such as raphides (needles), druses (spherical aggregates) or prisms. With some exceptions they are located within the plant body (in roots, stems, leaves, seeds). Their protective function against herbivorous animals has been discussed for a long time, but this function is still almost a question of the relation of sizes of both the herbivorous animal and the crystals [41.74].

The most common origin of cellular structuring is due to epicuticular waxes. Because of their importance as multifunctional interfaces, the morphological diversity of epicuticular waxes, their chemical diversity, and

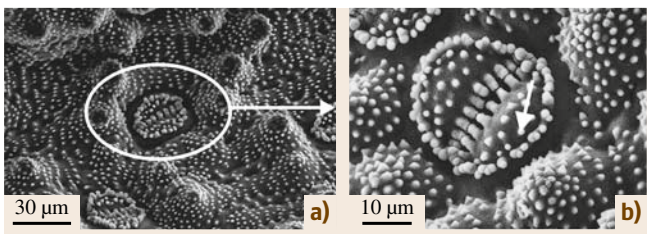

Equisetum arvense, silicon dioxide inserts are indicated by the *arrow* in (b)

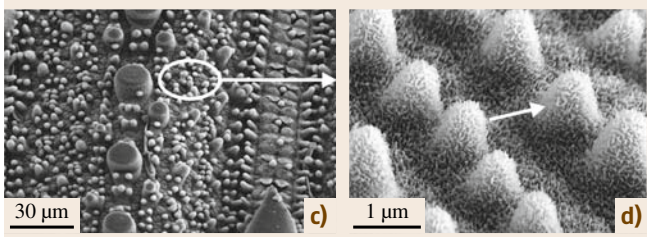

Oryza sativa, silicon dioxide inserts are indicated by the *arrow* in (d)

Fig. 41.15a–d Cell surface structuring by subcuticular silicon dioxide insertions. SEM micrographs of the common horsetail (*Equisetum arvense*) are shown in **(a,b)**. **(b)** Provides a detail of **(a)** and shows that the stomata and their surrounding cells have a micropattern of small enhanced spots formed by subcuticular inserts of silicon oxide crystals. In **(c,d)** the surface of *Oryza sativa* is shown. Here the convex sculpturing is also caused by subcuticular silicon oxide crystals

their origin by self-assembly is extensively introduced in Sect. 41.1.2.

Multicellular Surface Structures in Plants

The previous examples have shown that the large structural diversity in plants is caused by the different morphologies of the cells and their surface structures. The dimensions of these structures range from a few nanometers, e.g., wax films, to several micrometers in cells. However, on several plant surfaces, larger structures are multicellular; what that means is that more than a single cell is needed to form such structures. Several properties are correlated to multifunctional surface structures, and the most common are secreting glands and nonsecreting multicellular trichomes, which are introduced in the following.

Glands or glandular trichomes can be found on ≈ 30% of all vascular plants [41.75]. Multicellular glands include salt glands, nectaries, and the adhesive-secreting glands of some carnivorous plants [41.63]. Secretion and accumulation of toxic compounds at the plant surface allows direct contact with insects, pathogens, and herbivores, and might therefore be an effective defense strategy [41.63]. The exudates of glands are, for example, terpenoids, nicotine, alkaloids or flavonoids. The exudates of some ferns and angiosperms, in particular several members of the *Primulaceae*, are composed of flavonoids [41.76, 77]. These flavonoid exudates or *farina* are morphologically similar to waxes, but are chemically distinct from plant waxes. Other glandular trichomes, such as the glands of the carnivorous plants of the genus *Drosera* (sundew) and *Pinguicula* (butterworts), secrete adhesives and enzymes to trap and digest small insects such as mosquitoes and fruit flies.

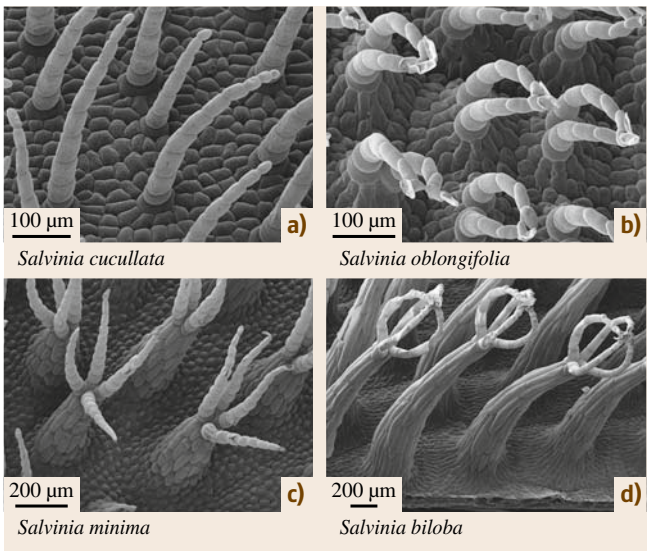

Fig. 41.16a–d SEM micrographs of four different multicellular hair types in the genus *Salvinia*. The *cucullata* type **(a)** is formed by solitary trichomes of up to 800 µm length and 50 µm in diameter. The *oblongifolia* type **(b)** is formed by groups of two trichomes, bending in the same direction and sitting on an emergence, with heights of up to 330 µm. The upper terminal (apical) cells are loosely connected. The *natans* type **(c)** is formed by four trichome branches, each elevated on a large emergence. The total height is approximately 1300 µm. The *molesta* type **(d)** is formed by four trichome branches on a large emergence, which are connected by their upper terminal cells. The height of these hairs reaches 2200 µm

Multicellular hairs are common in many flowering plant groups. Particular interesting forms occur in the floating water ferns of the genus *Salvinia*. Within this genus, morphologically different kinds of water-repellent (superhydrophobic) hairs exist. The multicellular hairs on the upper (adaxial) side of the leaves of the species of genus *Salvinia* form complex hierarchical surface structures which are able to retain an air layer at the surface, even when leaves were fixed underwater for several days [41.78, 79]. The hairs are multicellular, and their sizes are in the range of several hundred micrometers. Four different hair types have been described for the genus *Salvinia* [41.80]. The SEM micrographs in Fig. 41.16 show their morphological variability. Based on these morphological types, four groups, each with several species, have been formed. The *Cucullata* type (Fig. 41.16a) is characterized by solitary and slightly bent trichomes and occurs in *S. cucullata* and *S. hastate*. The *Oblongifolia* type (Fig. 41.16b) forms groups of two trichomes, which bend in the same direction and sit on an emergence. This type occurs on *S. oblongifolia*. The *Natans* type, shown in Fig. 41.16c, has four trichome branches, each elevated on a large multicellular base and in total has a height of up to 1300 µm. The heights of the trichome groups decrease towards the leaf margins. This type occurs in *S. natans* and *S. minima*. In the *Molesta* type (Fig. 41.16d) four trichome branches are grouped together, connected with each other by their terminal cells and sitting on a large emergence. The heights of the trichomes reach up to 2200 µm in *S. molesta*, but also decrease towards the leaf margins. This trichome type is characteristic of, e.g., *S. molesta* and *S. biloba*. In all these species, the epidermis is covered with small three-dimensional waxes in the

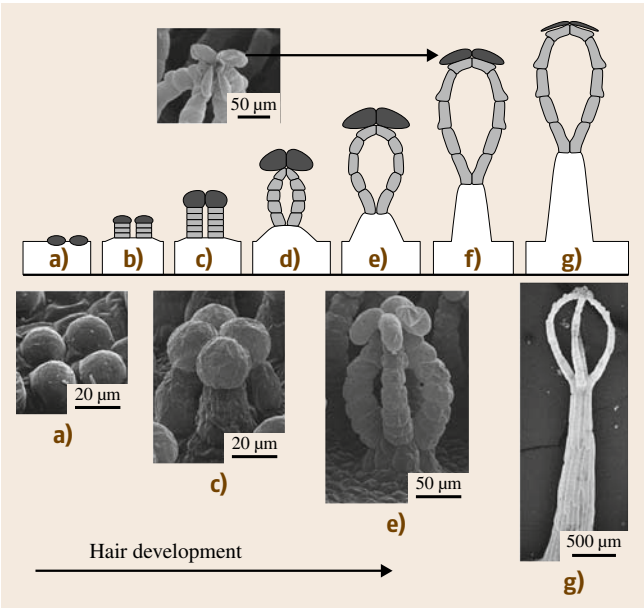

Fig. 41.17a–g Development of multicellular hairs in *S. molesta* on the upper side of the floating leaves. The schematic shows a side view (only two of four hair branches are shown) of the developmental stages during the formation of a crown-like hair. Four different developmental stages are shown in the SEM micrographs below. In this, the development starts by cell division below the four single cells shown in **(a)**. Continuous growth **(b–d)** results in a crown-like structure **(e)**. Further cell division leads to a multicellular hair **(g)** ▶

form of transversely ridged rodlets. The development of these complex structures, shown in Fig. 41.17, has been studied in *S. biloba* by *Barthlott* et al. [41.80]. In an early stage of leaf development, hair formation starts with a grouping of four cells, shown schematically in Fig. 41.17a. During the ontogeny of the leaf, four branches develop from these initial cells and form a crown-like structure (Fig. 41.17b–e) in which the single branches are connected with each other. Later, the base grows by cell division and cell expansion to develop a large base below the crown structure (Fig. 41.17f,g). These complex multicellular surface structures have been replicated by *Cerman* et al. [41.79], and replicas and leaves have been used to study the coherence of superhydrophobicity and air-retaining surfaces for drag reduction in underwater use (Sect. 41.2.4).

41.2 Multifunctional Plant Surfaces

Since the first plants moved from their aqueous environment to the drier atmosphere on land, plants have developed specific features for successful survival in nearly all conceivable habitats on Earth. Their adaptations have been selected by millions of years of plant evolution and include morphological, physiological, and structural specifications. Those features which were advantageous for the survival of individuals in their environment have been passed on from one generation to the next. Through natural selection, characteristics which are constitutionally present in the various groups of plants are amplified, intensified, and combined in various ways, yielding adaptation(s) to a particular habitat. However, some specific functional surface structures have evolved several times in nature; thus they exist in several groups of plants which are not closely related. Plant surfaces play an important role as interfaces to the biotic (living) and nonbiotic environment, thus it is not surprising that, in different plants and environments, a huge variety of functional surface structures have evolved.

41.2.1 Reflection and Absorption of Spectral Radiation

Temperature of plants in hot areas increases when the uptake of direct and indirect solar radiation is greater than heat transfer from the plant to the environment [41.81]. Plants usually reduce their temperature significantly by evaporation (transpiration) of water, but this mechanism of cooling requires regular uptake of water, which is limited in dry habitats. In dry areas, convective cooling is an important mechanism of heat transfer [41.82]. The latent heat flux from the vegetation to the environment depends largely on convection, which is correlated to leaf shape and size, and wind speed. Higher wind speeds cause turbulence in the plant boundary layer and force convection with mass flow [41.81, 83–85]. Most nonsucculent desert plants have small leaves which are expected to develop a small boundary-layer thickness and therefore have a high boundary-layer conductance for heat and mass transfer [41.83, 86]. However, many leaves and stem surfaces

are larger and therefore need a different mechanism of temperature control. In this regard, reduction of energy uptake is the most important way to reduce heat stress. The most common reflective structures on desert plants are three-dimensional waxes and a dense covering with air-filled hairs.

Spectral Properties of Plant Waxes

Waxes in many plants of dry habitats cause a bluish and white appearance of the plant surfaces. Leaves of some eucalyptus trees, as shown in Fig. 41.1g,h, show such a bluish surface structure and a dense layer of epicuticular waxes. The coloration results from the reflection of visible light, caused by surface structures in the dimensions of the wavelength of short-wave visible light, and by reflection of UV radiation [41.87–91]. Waxes on plant surfaces can reduce the uptake of radiation energy by reflection, and thereby control the temperature of the organisms [41.92]. Radiation emitted or reflected by plant surfaces occurs in the range from 280 nm to the infrared, including the wavelengths from 400 to 700 nm visible to the human eye [41.93]. Absorption of visible light is essential for photosynthesis, thus all leaf surfaces are translucent for the photosynthetically active wavelengths of solar radiation. However, intense solar radiation can depress the activity of photosynthesis, thus reflection of visible light is advantageous for desert plants to extend their photosynthesis [41.92, 94].

Three-dimensional waxes reflect a large part of the visible light, but can also play a significant role in the reflection of shortwave ultraviolet (UV) radiation [41.90]. The UV reflection of epicuticular waxes is caused by the dimensions of the waxes, which is similar to the wavelength of UV light (UV-B 280–320 nm and UV-A 320–400 nm) [41.87]. Furthermore, the epicuticular waxes of some species have been reported to contain UV-B-absorbing compounds [41.95]. Harmful ultraviolet radiation (280–400 nm) appears to be attenuated by phenols, in particular by cinnamic acids and by lipoidic flavonoids associated with the cuticular matrix or with the cuticular waxes [41.96, 97]. External flavonoid aglycones are found in various families throughout the higher plants, but occur very frequently in plants of (semi)arid habitats [41.98]. UV absorption is also important for plants growing in high altitudes in mountains, where significant UV levels can be found. UV-absorbing waxes of *Pinus mugo* subsp. *mugo* (dwarf mountain pine) contain chromophores that absorb UV radiation in such a way that it removes the most harmful UV-B and UV-A from the solar spectrum [41.99]. These fluorescent cuticular waxes remove the most damaging part of the UV radiation and convert it into harmless blue light. *Jacobs* et al. [41.99] suggest that the UV absorption and transformation found in plant waxes of *Pinus mugo* can be used for the development of new technological methods of protection against this harmful radiation.

Spectral Properties of Hairs

Besides three-dimensional waxes, the most common reflective structures on desert plants are a dense coverage with air-filled hairs. *Ehleringer* and *Björkman* [41.100] studied the spectral properties of *Encelia farinosa* leaves, which occur in different habitats. They showed that plants grown in drier areas have a denser and thicker hair layer. In *Encelia farinosa*, the hairs preferentially reflect near-infrared radiation (700–3000 nm) over photosynthetically useful solar radiation (400–700 nm). Such reflective properties have been found for several further species with a dense coverage of hairs, such as shown in Fig. 41.11a, by *Holmes* and *Keiller* [41.90]. Additionally such dense coverage of hairs may possibly increase the thickness of the leaf boundary layer, thus reducing the rate of water loss in water-limited habitats [41.85, 101]. Especially, the surfaces of plants from dry and hot environments show different microstructural adaptations to protect the plant from harmful radiation. The pubescence (presence of hairs) and glaucousness (presence of a thick epicuticular wax layer) are the two surface characteristics which have a marked effect on the total reflectance of plant surfaces in species of dry and hot habitats. However, the structural characteristics typical of plants of arid regions are frequently occurring structures, and therefore not exclusive to desert species.

41.2.2 Slippery Plant Surfaces

Many plants have evolved special structured surfaces which hinder the attachment of animals, especially insects, to protect themselves against herbivores [41.102]. Most insects possess two different types of attachment structures: claws and adhesive pads [41.103, 104]. Whereas the former are used to cling to rough surfaces, the latter enable them to stick to perfectly smooth substrates. One strategy to reduce the attachment of insects is the secretion of epicuticular waxes which assemble into three-dimensional microstructures. The other strategy is the development of a slippery surface by inducing aquaplaning.

Wax-Induced Slippery Surfaces

On a microrough wax layer, the use of both insect attachment structures mentioned above is impeded. On the one hand the wax crystals are too small and too fragile for the claw tips of insects to be inserted, and on the other hand the surface structure is too rough for the adhesive pads to develop sufficient contact area. Thus three-dimensional waxes can prevent walking of insects on the plant by the development of a slippery surface. The stems of many *Macaranga* plants (*Euphorbiaceae*) are covered by epicuticular wax crystals, rendering the surface very slippery for most insects, but specialist ants, which nest inside the hollow twigs of the plant, are able to walk on the waxy stem surfaces without any difficulty. The waxy surface is composed of long thin threads, which make the surface slippery for other ants and insects [41.105]. On these plants the wax acts as a selective barrier, protecting the symbiotic ant partners against competition from other ants.

Wax crystals on flower petals are extremely rare, because most pollinators must attach to the petal surfaces for pollination. However, in a special group of trap-flowers, insects are temporarily trapped into a flower trap, usually formed as a saccate structure (utricle) by the flower petals (perianths), for pollination. In this group, several species show waxy and slippery surface structures near the entrance of the trap-flower, and in some flowers the inner trap surface is also covered by wax, preventing the insect from climbing out. Such a waxy surface with large wax platelets is shown in Fig. 41.4f for *Aristolochia albida*. A comprehensive study of the surface structure in trap-flowers has recently been performed by *Poppinga* [41.106].

Some species of the carnivorous pitcher plants of the genus *Nepenthes* (Fig. 41.18a–e) use slippery wax layers in order to capture and retain insects. Carnivorous plants in the genus *Nepenthes* have pitcher-like leaves, formed as traps for catching and digesting insects. In these species, a layer of three-dimensional wax platelets creates a slippery zone inside the tube, above the digestive zone [41.107]. The wax plays a crucial role in animal trapping and prey retention. Insects are not able to attach to and walk on these waxy surfaces. They slide into the digestive fluid and are restrained from further escape. In *N. alata* the wax coverage consists of two overlapping layers; the upper layer is shown in the SEM micrograph in Fig. 41.18d. These layers differ in their structure, chemical composition, and mechanical properties. The upper layer is the one that comes into contact with the feet of insects. In this layer the waxes are less mechanically stable, and break easily at their smaller stalked bases into small pieces when insects slide over them. These broken wax particles adhere to the adhesive pads of insect feet (tarsi). The remaining lower wax layer provides an already rough surface structure, which reduces the adhesion area for the insect pads. Thus insect sliding is induced by a decrease in the attachment force of insects by two different mechanisms: first, by contamination of insects' attachment organs, and second, by reduction of the real contact area [41.108].

Aquaplaning on Plant Surfaces

There are several *Nepenthes* species which do not possess a waxy layer, but are nevertheless fully functional insect traps. It was found that *Nepenthes* evolved another capture mechanism which is based on special surface properties of the pitcher rim (peristome) (Fig. 41.18a,b). The peristome is characterized by a regular microstructure with radial ridges of smooth, overlapping epidermal cells, which form a series of steps towards the pitcher inside. The peristome ridges (Fig. 41.18c) mostly extend into tooth-like structures at the inner edge, in between which large glands (ex-

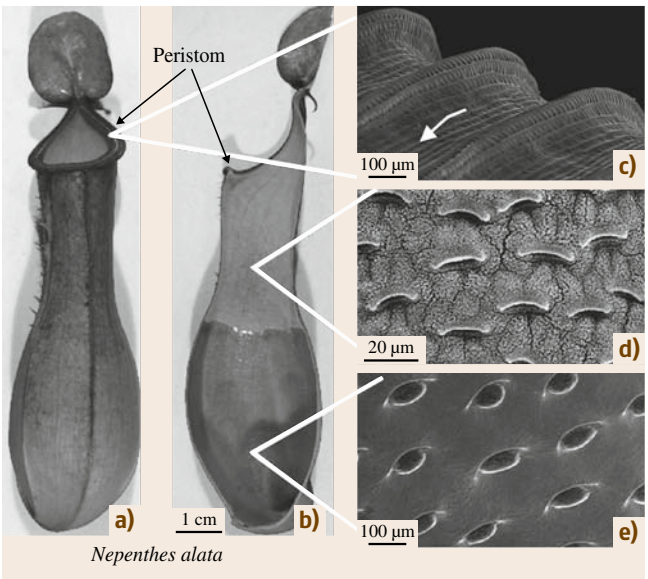

Fig. 41.18a–e Pitcher traps of the carnivorous plant *Nepenthes alata*. In **(a)** the complete pitchers trap of *N. alata* and in **(b)** a longitudinal cut through the trap are shown. **(c)** Shows parallel ridges of the hydrophilic peristome. The *arrow* indicates the direction toward the inside of the pitcher (courtesy Holger Bohn). In **(d)** the waxy and slippery surface inside the trap, with inactive stomata, is shown. In **(e)** glands located in the digestive zone at the lower part of the trap are shown

trafloral nectaries) are situated. Secretion of nectar by these glands attracts small insects, but leads also to a hydrophilic coverage of the surface. The plant surface microstructure, combined with hydrophilic surface chemistry, renders the pitcher rim completely wettable. Water droplets spread rapidly and form homogeneous thin films, which make the peristome extremely slippery for insects. When the peristome is wet, the fluid films prevent the insects' tarsal adhesive pads from making close contact with the surface, similar to the aquaplaning of a car tire on a wet road. In addition, the anisotropic microstructure of the peristome surface allows interlocking of claws only while the insect is running towards the pitcher inside, but not on the way out [41.109]. Under natural conditions the slippery water films are caused by rain, condensation, and nectar secretion. In contrast to this, dry peristomes are not slippery for insects. This weather-dependent variation of peristome slipperiness leads to intermittent and unpredictable activation of *Nepenthes* pitcher traps, which might make the evolution of specific avoidance behaviors more difficult [41.110].

41.2.3 Wettability and Self-Cleaning of Plant Surfaces

Basics of Surface Wetting

Wetting is the fundamental process of liquid interaction at solid–gaseous interfaces. It describes how a liquid comes into contact with a solid surface. Wetting is important in many everyday situations, for example, liquid painting on walls, printing of texts, and in the transport of fluids (water, oil, blood, and many others) through pipe systems, and it is the basis of several cleaning procedures. However, there are many situations where it is desirable to minimize wetting; water droplets adhering to window glass and car windshields reduce visibility and leave residuals after evaporation, rainwear should stay dry even during heavy showers, and movement of boats in water costs extra energy because of friction force at the interfaces. Wetting is also important for many biological processes such as the germination of seeds or microorganisms such as fungi, and reproduction of bacteria, and is essential for water uptake in soils. Under suitable conditions, microorganism proliferation results in the formation of larger populations called biofilms. Biofilms induce apparent defects in technical materials, and also their acidic excretions are damaging to buildings and technical materials [41.111]. Thus, it is not surprising that the basics of surface wetting processes have been of scientific interest for several decades and a large amount of scientific work has been carried out to understand and produce surfaces which are extremely water repellent. The basics of surface wetting are summarized here. For a deeper study, specific literature such as the books by *Israelachvili* [41.112], *Bhushan* [41.113], *De Gennes* et al. [41.114], and *Bhushan* [41.115] are recommended.

Surface Wetting and Contact Angle. A droplet on a solid surface wets the surface to a greater or lesser extent that is dependent on the contact angle (CA). A high contact angle describes surfaces on which a water droplet forms a spherical shape; thus the real contact between the adhering droplet and the surface is very small compared with wettable surfaces, on which an applied drop of water tends to spread, and the contact angle is low. The CA of a liquid on a surface depends on the surface tension (molecular forces) of the involved liquid, solid surface, and the surrounding vapor. Thus, wetting depends on the ratio between the energy necessary for the enlargement of the surface and the gain of energy due to adsorption [41.112, 116]. The basis for studying equilibrium wetting on rough surfaces was established many years ago by *Wenzel* [41.117] and *Cassie* and *Baxter* [41.118]. The Wenzel equation expresses a general amplification of the wettability induced by roughness and applies to a CA where droplets are in equilibrium, but not to advancing and receding angles of a droplet on a rough solid surface that give rise to contact-angle hysteresis (CAH) as shown in Fig. 41.19. Hysteresis is responsible for the sticking of liquids on a surface, and is defined as the difference of the advancing and receding angles of a moving or evaporating water droplet ($\mathrm{CAH} = \mathrm{CA_{adv}} - \mathrm{CA_{rec}}$). If additional liquid is added to a sessile drop, the contact line advances; if liquid is removed from the drop, the CA decreases to a receding value before the contact retreats. If a droplet moves over a solid surface, the CA at the front of the droplet (advancing CA) is greater than that at the back of the droplet (receding CA). However, if the droplet rolls with little resistance, the contact angle hysteresis is small.

On water-repellent surfaces, an applied droplet starts to roll off the surface when it is tilted to a specific angle. This tilt angle (TA) is simply defined as the tilting angle of a surface on which an applied drop of water starts to move. Low TA ($< 10°$) is characteristic of superhydrophobic and self-cleaning surfaces. Another important phenomenon related to wetting behavior is the bouncing of droplets. When a droplet hits a surface,

it can bounce, spread or stick. In practical applications of superhydrophobic surfaces, surfaces should maintain their ability to repel penetrating droplets under dynamic conditions [41.119, 120].

Definition of Surface Wetting Contact Angle and Hysteresis. Contact angle measurement is the main method for characterization of the hydrophobicity of surfaces, and the CA is a measuring unit for the wettability of surfaces. The wetting behavior of solid surfaces can be divided into four classes, defined by their CA, and for superhydrophobic ones, also by their hysteresis. On wettable surfaces with low contact angles, a fluid will spread and cover a larger area of the surface. Such surfaces are termed superhydrophilic when the CA is $< 10°$. Surfaces with CAs of $\geq 10°$ and $< 90°$ are termed hydrophilic surfaces. Unwettable surfaces have high contact angles, meaning the liquid on the surface forms a hemispherical or spherical droplet. Surfaces on which the CA is $\geq 90°$ and $< 150°$ are termed hydrophobic. A superhydrophobic surface is defined as one that has a static CA of $\geq 150°$, and if those superhydrophobic surfaces have a low hysteresis or a low tilting angle of less than $< 10°$ they are superhydrophobic and can provide self-cleaning properties. This definition of superhydrophobic surfaces has been used in most recent reviews [41.120–124] and is the preferred one which might be used to overcome the existing variety of definitions.

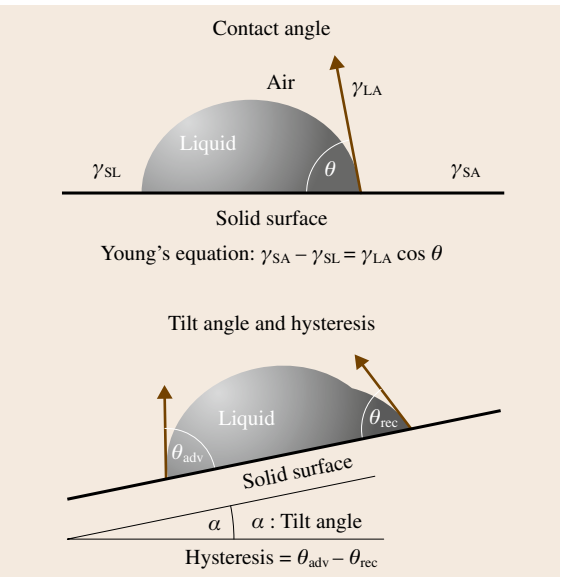

Fig. 41.19 Wetting of a solid surface with water, with air as the surrounding medium; γ_{LA}, γ_{LS}, and γ_{SA} are the interfacial tensions at the corresponding boundaries between liquid (L), solid (S), and air (A), which determine the CA of an applied water droplet, described by Young's equation. The hysteresis of a water droplet on a tilted surface represents the adhesion of the liquid on the surface and can be determined by measuring the tilting angle or the advancing and receding angle of a water droplet

Wetting of Plant Surfaces

The plant cuticle with its integrated and exposed waxes is in general a hydrophobic material, but structural and chemical modifications induce variations in surface wetting, ranging from superhydrophilicity to superhydrophobicity. Plant surface wetting is influenced by the sculptures of the cells, such as the formation of hairs, and by the fine structure of the surfaces, such as folding of the cuticle, or by epicuticular waxes. Representative plants and their structures and wettability are given for the four defined classes of surface wettability (hydrophobic, hydrophilic, superhydrophobic, and superhydrophilic). The different structural characteristics of plant surfaces and their wetting behavior are summarized in Fig. 41.20, and examples are given below.

Hydrophilic and Superhydrophilic Surfaces. On hydrophilic surfaces, a drop of water has a contact angle between $\geq 10°$ and $< 90°$. Hydrophilic surfaces are known from many leaves which have a papilla cell morphology and cuticular folding, but also from leaves with flat, tabular cells. Those leaves have only smooth wax films on their surface and no or only isolated three-dimensional wax crystals. Examples are shown in Fig. 41.14. Other hydrophilic surfaces have trichomes (hairs and glands) on their surface. On hydrophilic surfaces hairs are not covered with three-dimensional (3-D) waxes, which would make the surfaces hydrophobic. Examples are shown in Fig. 41.11. Glands influence the wettability of surfaces by their secretions, which can be very hydrophilic, as mentioned above for the nectar-secreting glands in *Nepenthes* and the water-spreading leaves of *Ruellia devosiana* [41.3]. However, why are the petals of most flowers hydrophilic? The explanation for this phenomenon is given by the functions of flower petals. In most plants, petals are developed to attract pollinators, in most cases small insects, and these pollinators must be able to walk on the petal surfaces. Thus, a coverage with three-dimensional waxes, which reduces the adhesion of most insects, would be disadvantageous. Additionally, it is important to notice that hydrophobic leaves might become hydrophilic by

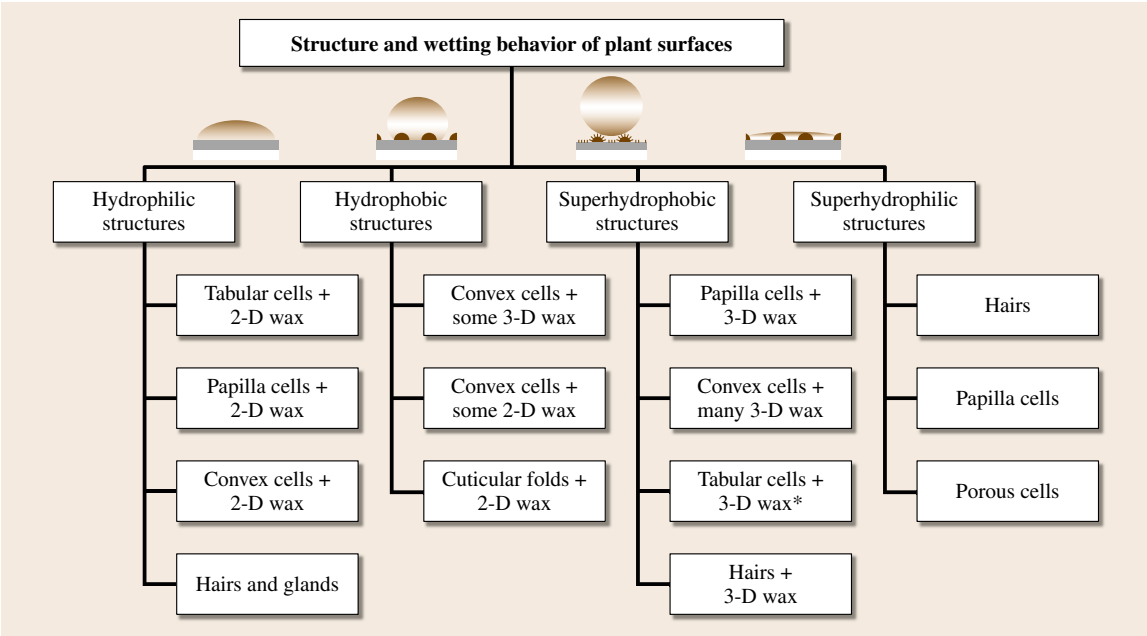

Fig. 41.20 Four groups of wettability of plant surfaces and the possible surface structures and structure combinations. The wetting drawings used for the four groups are correlated to specific contact angles. Both the hydrophobic and superhydrophobic surfaces can be built by convex cells with three-dimensional waxes on them, but only a dense layer (many wax crystals per area) leads to superhydrophobic surfaces (**Neinhuis* and *Barthlott* [41.17] defined these as temporary superhydrophobic surface structures, because erosion of 3-D waxes by environmental impacts can damage the waxes and decrease the contact angle)

the accumulation of environmental, hydrophilic contaminations such as spores, bacteria, dirt particles, and chemical aerosols on their surfaces. Atmospheric particles are mostly a conglomerate of different salts and organic materials [41.125]. These salts dissolve in rain, fog, and dew, or may become dissolved by stomatal transpiration of the leaf [41.126] and increase the hydrophilicity of plant surfaces [41.127].

Superhydrophilic surfaces are characterized by the spreading of water on the surface. Contact angles of such surfaces are, if measurable, 10° or less. Superhydrophilicity is based on different morphological structures, and by the chemistry of the surface, e.g., through secretion of hydrophilic compounds by epidermal glands. Optimized organs for the uptake of water are the roots of plants. Most roots are characterized by papillae and hairy cells, but porous surface structures have also been described for air roots of epiphytic plants. Superhydrophilicity is a great advantage for lower plants (a collective term for three groups of plants: the mosses, liverworts, and lichens), which have no roots for water uptake and no vascular system for water transport. Some species have not even developed a waxy cuticle as a transpiration and stabilization element. Water uptake and the uptake of nutrients in many lower plants occurs over the complete surface. Peat moss (*Sphagnum*) belongs to the lower plants and is common in wet swamps and mires, where it might represent the dominant biomass. The complete plant surface is free of stomata, which function in higher plants for water transpiration control. Water uptake and gas exchange occurs via pores, shown in Fig. 41.21a, which are spread over the plant body. Pores are relatively large openings of 10–20 μm in diameter, whereas the openings of a porous surface texture with openings of 0.2 μm and less are much smaller. An example of a water-absorbing porous cell surface structure is given by the leaf surface of the moss *Rhacocarpus purpurescens*. The superhydrophilic surface of *R. purpurescens* is shown in the SEM micrographs presented in Fig. 41.21b. The functional characteristic of the surface structure of the leaves of this moss is rapid absorption of fog, dew or rain [41.128, 129]. Water absorption via the plant surface is not limited to lower

plants. In higher plants, all specimens of the *Bromelia* family, e.g., pineapple (*Ananas comosus*) or Spanish moss (*Tillandsia usneoides*) (Fig. 41.21c,d), have water-absorbing, multicellular absorptive trichomes on the epidermis cells. Some genera in this group form funnels by arranging their leaves in the form of a rosette. In these funnels, water can be stored after a rain shower and organic litter can accumulate and decay, so hairs at the funnel surface also absorb nutrients dissolved in the water. Further water-absorbing structures are porous thorns in some cacti, which absorb water condensed at the surface [41.1]. Some leaves of tropical plants, such as as those of *Ruellia devosiana* [41.3], *Marantha leuconeura*, and *Calathea zebrina*, are also superhydrophilic. The latter ones show strong convex sculpturing of their epidermis cells, but little information about the physicochemical basis of superhydrophilicity and the biological advantage of these properties is available.

It can be summarized that, in some lower plants and the species of the *Bromeliaceae*, superhydrophilic surfaces have evolved for water and nutrient uptake. However, a water film on the surface can reduce uptake of CO_2, which is required for photosynthesis [41.62]. On wet surfaces the growth of most pathogen microorganisms, including bacteria and fungi, is provided by permanent or temporary water availability. Additionally, lensing effects of water droplets on leaf surfaces can increase incident sunlight by over 20-fold directly beneath individual droplets [41.62], which may have important implications for processes such as photosynthesis and transpiration for a large variety of plant species. Thus, there may be strong selective pressure for increased water repellency in terrestrial plant leaves.

Hydrophobic and Superhydrophobic Surfaces. The chemical constituents of most plant surfaces are hydrophobic, meaning that a water droplet applied to the surface has a static contact angle between $\geq 90°$ and $< 150°$. This phenomenon is based on the hydrophobic waxy nature of the plant cuticle, the primary function of which is as a barrier against water loss. The micromorphological characteristics of hydrophobic plant surfaces are tabular cells or only slightly convex epidermal cells, covered with a thin wax film (2-D waxes) or by a relatively low amount of 3-D waxes. Additionally, tabular cells might be structured by cuticular folding, and then a 2-D wax layer is present on the surface. However, for most plants, these wax layers have not been observed, because they are not or are only rarely visible in SEM. It might also be that a hairy leaf surface forms

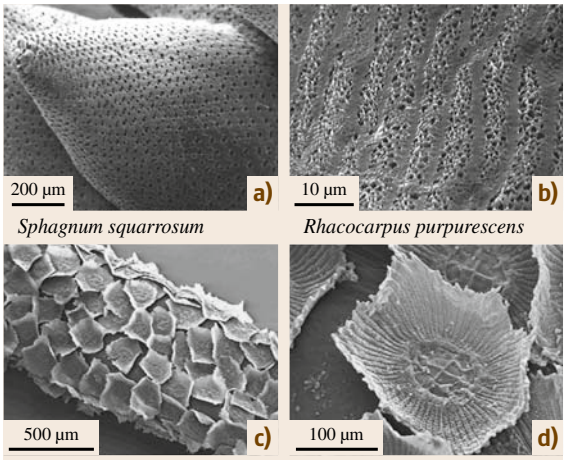

Fig. 41.21a–d SEM micrographs of superhydrophilic plant surfaces. In **(a)** the water uptake pores of a *Sphagnum squarrosum* moss and in **(b)** the water-adsorbing porous surface of the moss *Rhacocarpus purpurescens* are shown. In **(c)** the epiphytic-growing Spanish moss (*Tillandsia usneoides*) is shown. Figure **(d)** shows a higher magnification of the water-absorbing hairs of *T. usneoides*

hydrophobic structures, but evidence with given contact angles has not been found; thus, we forego adding these structures to the more frequent surface morphologies.

Many leaf surfaces are superhydrophobic, as demonstrated by *Neinhuis* and *Barthlott* [41.17], who investigated over 200 water-repellent plant species. As defined above, a surface is termed superhydrophobic when the static CA is equal to or above 150° and low hysteresis lets a water droplet roll off at surface inclinations below 10°. The morphological characteristics of superhydrophobic leaves in most cases are a hierarchical surface structure, formed by convex to papillose epidermal cells, and a very dense arrangement of three-dimensional epicuticular waxes of different shapes. In Fig. 41.22 three species with such hierarchical surface structures are shown. All known crystal forms were found on superhydrophobic leaves, and their size ranged from 0.5 to about 20 µm in length [41.6]. Based on these investigations, it has been concluded that the superhydrophobicity of most plant surfaces is achieved by hierarchical structures of convex or papilla epidermal cells with three-dimensional wax structures on top.

It has also been found that tabular cells with a dense arrangement of wax crystals are superhydrophobic (e.g., *Brassica oleracea* and *Crambe maritima*), but those

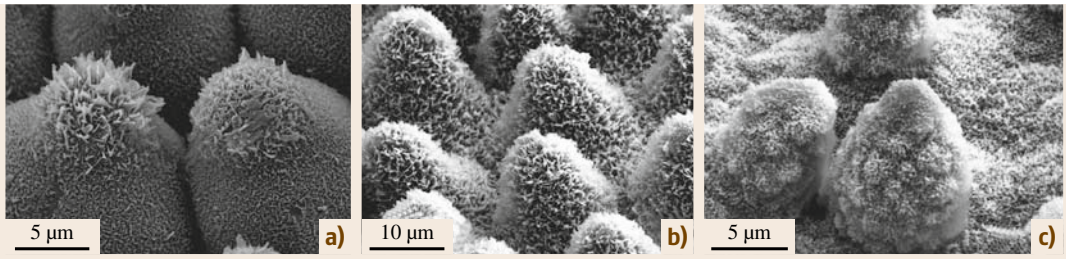

Fig. 41.22a–c SEM micrographs of the hierarchical structures of superhydrophobic leaves of **(a)** *Colocasia esculenta*, *Euphorbia myrsinites*, and *Nelumbo nucifera* (lotus). Leaves of all three species are characterized by convex **(a)**,**(b)** to papillose **(c)** cells, with coverage of three-dimensional wax crystals

leaves are water repellent for only a limited period of time. This, in most cases, is when leaves are in development and wax biosynthesis is active, but on mature leaves damage or erosion of the waxes can influence the wax structure and result in a less hydrophobic surface.

Besides the superhydrophobic leaf structures described before, a second method of water repellency has been developed in plants. Hairy leaf surfaces, such as those on the leaves of the lady's mantle (*Alchemilla vulgaris* L.) can very efficiently repel water. On such surfaces, a deposited drop bends the fibers (hairs), but the stiffness of the hairs prevents contact with the substrate, and promotes a fakir state of the water droplet [41.130]. The hydrophobic hairs of the water fern *Salvinia*, which have been introduced before and are shown in Figs. 41.16 and 41.17, are also superhydrophobic [41.79]. The use of these biological structures for the development of biomimetic air-retaining surfaces will be discussed in detail later. Superhydrophobic hairy surface structures are also known from animals, for example, water beetles and the water spider. These hairy systems may also be extremely useful for underwater systems because they minimize the wetted area of immersed surfaces and therefore may greatly reduce drag, as well as the rate of biofouling. Therefore, underwater superhydrophobicity is of great interest in biomimetics and is discussed in more detail later.

Hierarchical Structures for Superhydrophobicity and Self-Cleaning

The self-cleaning ability of microstructured, superhydrophobic plant surfaces was first described by *Barthlott* and *Ehler* [41.59], and the large shield-shaped leaves of the sacred lotus plant (*Nelumbo nucifera*) show this phenomenon to perfection [41.6]. Without knowledge of the physicochemical basics of self-cleaning, lotus has been a symbol of purity in Asian religions for over 2000 years [41.131]. Even emerging from muddy waters it unfolds its leaves unblemished and untouched by pollution. The hierarchical (double-structured) surface is characteristic of the lotus leaf and several other superhydrophobic leaves [41.17]. On lotus leaves the composite or hierarchical surface structure (Fig. 41.23) is built by convex papilla cells and a much smaller superimposed layer of hydrophobic three-dimensional wax tubules. The arrangement of the papilla cells is irregular, and orientation of the wax tubules is random. Wetting of such surfaces is minimized, because air is trapped in the cavities of the convex cell sculptures, and the hierarchical roughness enlarges the water–air interface while the solid–water interface is reduced. Water on such a surface gains very little energy through adsorption and forms a spherical droplet (Fig. 41.23), and both the contact area and the adhesion to the surface are dramatically reduced [41.6]. For lotus leaves the static contact angle is about 160° and the tilting angle $< 4°$.

The leaves of lotus (*Nelumbo nucifera*) are superhydrophobic and anti-adhesive with respect to particulate contaminations; thus contaminant particles are carried away by water droplets, resulting in a cleaned surface, as shown in Fig. 41.23a–c. A particle on a structured surface is like a fakir on his bed of nails, and the contact area and physical adhesion forces between a particle and the underlying leaf surface are considerably reduced. If water rolls over such a structured hydrophobic surface, contaminating particles are picked up by the water droplets, or they adhere to the surface of the droplets and are then removed with the droplets as they roll off. The reason for this is that only weak van der Waals forces bind the particle to the surface [41.132], whereas much stronger capillary forces between the particle and an adhering water droplet oc-

cur [41.119, 133, 134]. Thus, self-cleaning occurs on superhydrophobic leaves on which water moves over the surface to remove particles. Self-cleaning was found to be a result of an intrinsic hierarchical surface structure built by randomly oriented small hydrophobic wax tubules on the top of convex cell papillae (Fig. 41.23d–f). This self-cleaning process is independent of the chemistry of the adhering particles, i. e., whether they are hydrophilic or hydrophobic, and results in a smart protection against particle accumulation and is also a protection against plant pathogens such as fungi and bacteria [41.6, 17, 135]. In 2000, the trademark Lotus-effect was registered to label self-cleaning products based on the model of the lotus.

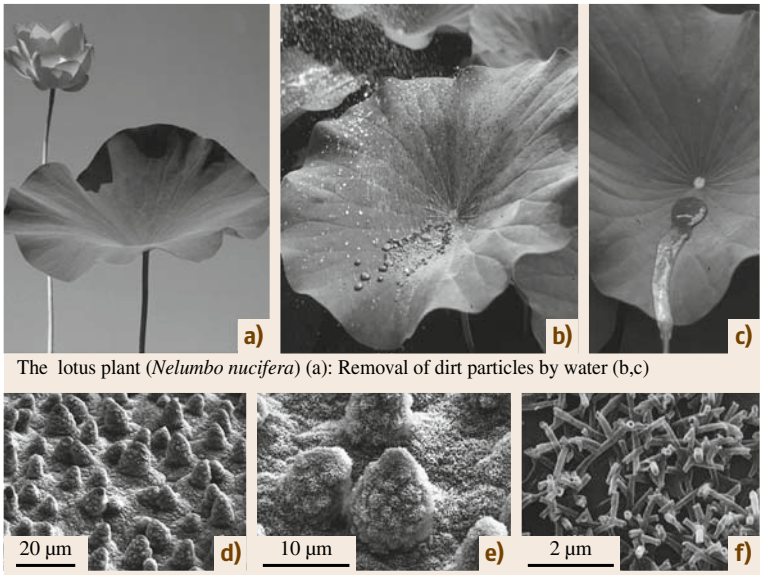

The lotus plant (*Nelumbo nucifera*) (a): Removal of dirt particles by water (b,c)

SEM micrographs of the lotus leaf (d) show the papillose cells (e) and wax tabules (f) on it

Fig. 41.23a–f Superhydrophobic and self-cleaning surface of lotus (*Nelumbo nucifera*). A flowering plant of lotus **(a)**, a lotus leaf contaminated with clay **(b)** and removal of the adhering particles by water **(c)**. The SEM micrographs **(d–f)** show the lotus leaf surface at different magnifications: **(d)** shows randomly distributed cell papilla, **(e)** shows a detail of the cell papilla, and in **(f)** the epicuticular wax tubules on the cells are shown

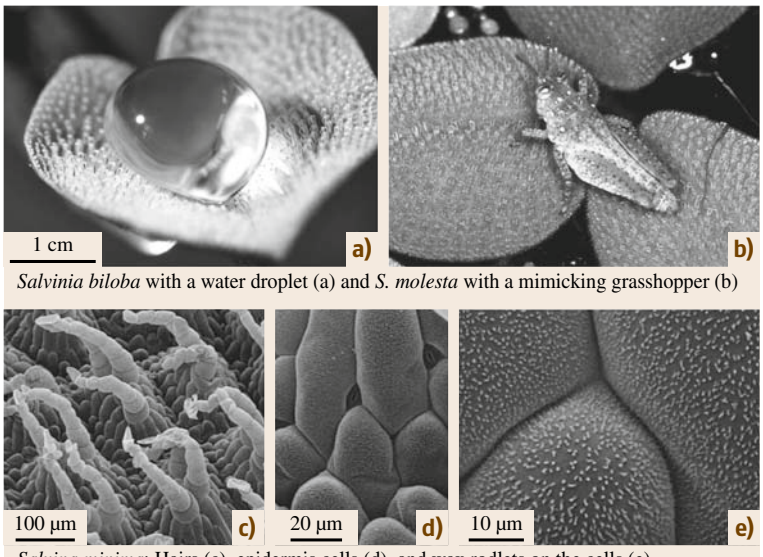

Salvinia biloba with a water droplet (a) and *S. molesta* with a mimicking grasshopper (b)

Salvina minima: Hairs (c), epidermis cells (d), and wax rodlets on the cells (e)

Fig. 41.24a–e Air-retaining surfaces of the water fern *Salvinia*. In **(a)** a water droplet on the upper leaf side of *Salvinia biloba* and in **(b)** a mimicking grasshopper on the leaf surface are shown. The SEM micrographs **(c–e)** of the leaf surface of *Salvinia minima* show the multicellular hairs **(c)**, and at higher magnification the epidermis cells **(d)** and the wax rodlets **(e)** on the epidermis cells

41.2.4 Superhydrophobic Air-Retaining Surfaces

Trichomes in general have a strong influence on leaf wettability. *Neinhuis* and *Barthlott* [41.17] found that the wettability of hairy leaves strongly depends on the presence or absence of wax crystals on the trichome surface. Leaves with nonwaxy trichomes were only water repellent for a short time after a water droplet had been applied. In contrast, leaves with waxy trichomes were extremely water repellent, for example, the leaves of *Salvinia auriculata* and *Pistia stratiotes*. The different types of hairs of *Salvinia* leaves have been introduced before. These surfaces are superhydrophobic (Fig. 41.24a), but the water droplets do not penetrate between the hairs; thus small particles from the leaf surface will not be removed by rinsing with water. However, a study by *Cerman* [41.79] showed that *Salvinia* surfaces are able to retain an air film for up to 17 days when positioned underwater. The crucial factor for superhydrophobicity in *Salvinia* leaves is the hairs, which are several hundred micrometers high and covered by hydrophobic wax crystals (Fig. 41.24c–d). These leaves, as well as their technical replicas, are air retaining and stay dry for several days when placed underwater.

Water plants developed such air-retaining surfaces to float on the water. As a result of coevolution, also insects such as younger nymphs of the semiaquatic grasshopper *Paulinia acuminata* (Fig. 41.24b) show similar structures by mimicking the effective surface texture of the leaves [41.136]. The surface adaptation of the grasshopper is an optical and functional mimicry, which means that the coloration and pattern of colors of the grasshopper mimic the fern's surface texture, and its waxy surface provides water repellency [41.136].

41.3 Technical Uses of Superhydrophobicity

Biological surfaces are evolutionary optimized interfaces and provide a large diversity of structures and functions. Wetting phenomena, as described for lotus leaves, and several other biological surface phenomena are based on physicochemical factors and therefore are transferable to technical surfaces.

41.3.1 Biomimetic Surfaces

Bionics or *biomimicry describes a process in which the ideas and concepts developed by nature are taken and implemented into technology* [41.137]. Biomimetic research deals with the analysis, extraction, and transformation of biological structures, materials, processes, and principles into technical use, and is of great interest for the design of modern functional innovative materials. Bionics contains a wide spectra of research fields, for example, lightweight constructions, fluid dynamics, robotics, micro- and nanoelectromechanical systems (MEMS, NEMS), and sensors. The dimensions of interest encompass the range from the molecular level up to the function of complex organisms. However, even if nature has successful solutions, these are not necessarily optimal for technical performance. It is very important to get a profound understanding of the principles of nature's solutions, by analyzing the functions and boundary conditions, in order to transfer them into artificial systems.

The first prominent example of successful transfer of biological surface structures is the drag-reducing surface structure of shark skin and the artificial surfaces (rippled foils) developed after this model [41.138]. Recently, the structure of shark skin has been used as a model for the development of swimming suits with reduced surface drag when diving in water [41.139]. The description of superhydrophobic and self-cleaning plant surfaces by *Barthlott* and *Neinhuis* in 1997 [41.6] can be interpreted as a stimulating moment for many scientists to focus research on functional biological surfaces [41.140, 141]. Prominent examples are the development of superhydrophobic surfaces after the model plant lotus [41.54, 55, 122, 123]. Other biological models are the feet of several arthropods and some vertebrates with their remarkable ability of reversible attachment to varying surfaces [41.142–144]. Remarkable adhesion systems can also be found in plants. The climbing shoots of ivy (*Hedera helix*) adhere to smooth and rough surfaces by the secretion of organic glue, which forms nanoparticles that allow aerial roots to affix to a surface [41.145]. Another bioinspired attachment system is the hook-and-loop fastener, which plants use for the dispersal of their seeds by attaching fruits to animals. Self-repairing processes in plants that seal fissures served as concept generators for the development of biomimetic coatings for membranes of pneumatic structures [41.146]. These are only

a few biomimetic examples; comprehensive overviews are given by *Benyus* [41.48], *Forbes* [41.141], and *Bar-Cohen* [41.147].

41.3.2 Structural Basics of Biomimetic Superhydrophobic Surfaces

Much theoretical and experimental work has been done to understand the physicochemical basics of superhydrophobicity. In this, several plants and their surface structures have been investigated. The structural parameters of the hierarchical surfaces and their influence on water and methanol repellency for 33 water-repellent plants has been studied by *Wagner* et al. [41.148]. This study showed that wax crystals of sizes from 0.5 and 5 μm had no significant influence on the hydrophobicity of the surfaces, but repellency increased when the aspect ratio of the cells increased. *Wagner* et al. [41.148] also characterized the number, height, and average lateral distance of papillae per unit area of six species with superhydrophobic surfaces. Even when papillae density varied between 737 and 3431 mm^{-2} and cell aspect ratios ranged from 0.8 to 0.5, no statistically significant variations in superhydrophobicity were found. However, a higher amount of smaller papillae seems to be more effective in terms of water repellency compared with surfaces with larger but fewer papillae. In this study also AFM and confocal light microscopy were used to calculate the solid–liquid contact area during wetting, and it was found that roughening on two hierarchical levels results in a reduction of the contact area between a water droplet and the plant surface of more than 95%. The influence of the wax nanostructures on the wettability of lotus leaves has been investigated by *Cheng* et al. [41.149]. In this, removal of the wax structure reduced the static contact angle from 146° to 126° (dry lotus leaf with molten wax), and hysteresis allowed water drops to adhere, even at tilting angles of 90°. This promising experimental approach did not change the chemistry of the surface, but led to a dramatic reduction of the cell aspect ratio by shrinkage of the cells.

Superhydrophobicity of hierarchical plant surface structures has been theoretically postulated earlier by *Otten* and *Herminghaus* [41.130] and was also confirmed by *Nosonovsky* and *Bhushan* [41.6, 150]. *Extrand* [41.151] investigated the interaction of capillary forces and gravity for a single asperity to suspend a liquid drop. In this, a microstructured surface was modified with a secondary structure by adding notches with sharp edges. It was stated that, if an asperity has a hierarchical structure, the secondary features can greatly enhance the surface repellency. *Marmur* [41.152] carried out theoretical analysis of the underlying mechanisms of superhydrophobicity and indicated that nature uses metastable wetting states as the key to superhydrophobicity. He concluded that the specific shape of the lotus leaf protrusions (cell papilla) lower the sensitivity of the superhydrophobic state to the protrusion distances. In these calculations simple parabolic shapes were used to simulate the morphology of the lotus cell papilla, but the influence of the secondary-level structure on the wetting behavior of the surfaces was not addressed.

For self-cleaning of superhydrophobic surfaces, a low hysteresis of less than 10° tilting angle is required. The degree of hysteresis is correlated with the wetting state of a liquid on a surface. On rough surfaces, an applied water droplet in the Wenzel state creates a wet contact mode with high hysteresis. In the Cassie state, the droplet sits on top of the structure asperities, hysteresis is low, and liquids roll off at low inclination angles. The intermediate wetting state occurs when the droplet sinks partially into the surface structures, but cavities of the surfaces are still air filled. Further wetting states with a high static contact angle, but also a high adhesive force (high hysteresis), have been described and called the Gecko wetting state [41.153] and petal effect [41.154]. However, these phenomena still seem to need more explanation before they can be accepted as new classifications of wetting states of superhydrophobic surfaces. *Li* and *Amirfazli* [41.155] combined theoretical calculations with experimental data by analyzing the thermodynamics of surface wetting of different surface textures (pillar height, width, and spacing). These calculations showed that small pillar spacing is needed for composite wetting states (Cassie state), whereas large pillar spacing is needed for large stable CA. Thus for achievement of large CA and small CAH simultaneously, a compromise between pillar spacing and other geometrical parameters such as pillar height, and spacing is necessary. *Nosonovsky* and *Bhushan* [41.150, 156–158] demonstrated that the effect of roughness on wetting and also the mechanisms that lead to destabilization of a composite interface are scale dependent. They concluded that multiscale roughness based on tightly packed convex papillae (asperities) with *nanobumps* as well as a hydrophobic nature of the material is optimum for superhydrophobicity. Optimal parameters for the development of stable, superhydrophobic rough surfaces have been calculated,

and their requirements for optimal superhydrophobic surfaces fit well with the already realized biological water-repellent lotus leaf surfaces with hierarchical structures.

41.3.3 Generation of Biomimetic Superhydrophobic Surfaces

Plant surfaces and their properties stimulated the development of new functional biomimetic surfaces and materials, and many investigations have been made into creating superhydrophobic surfaces. In the past, several new methods for surface functionalization have been developed, and special interest has been given to techniques for the development of superhydrophobic surfaces [41.123]. Hierarchical surfaces are the preferred structures for highly water-repellent surfaces [41.151, 155, 159]. The generation of superhydrophobic surfaces includes bottom-up techniques, in which the desired structures are built up from small units such as single molecules, and top-down techniques, in which a structure is applied to a material by, e.g., lithography or molding. Templating, a top-down technique, is a simple and fast technique for replication of surface structures. In this, a master surface is used as the template and is pressed or printed onto a material or a liquid is filled in. Lithography is a technique to produce precise geometric structures with different aspect ratios (height to width) on scales from a few nanometers to several micrometers.

Bottom-up approaches to fabrication use chemical or physical forces operating at the nanoscale to assemble basic units into larger structures. Thus, the synthesis of a micro- or nanostructured material starts at the atomic or molecular level. In this procedure the precursor particles grow in size by chemical reactions or self-assembly [41.160]. Chemical self-assembly is a technique to exploit selective attachment of molecules to specific surfaces. Nanostructures of a wide range of materials, including organic and biological compounds, inorganic oxides, and metals, can be processed using chemical self-assembly techniques. In chemical self-assembly the binding between the units is covalent, whereas the binding in self-assembly is noncovalent. Materials which have been used to create superhydrophobic surfaces by self-assembly of the material are metals and metal oxides such as silver aggregates, cobalt hydroxide, CuS-coated copper oxide, and ZnO nanorods. For references and further examples, see *Roach* et al. [41.123]. For the development of nano- and microstructures it is important to control structure sizes, shapes, and the distribution of structures, e.g., single particles or the formation of particle agglomerations.

In plant surfaces, the secondary level of superhydrophobic hierarchical structures is built up by three-dimensional waxes, whose different morphologies originate by self-assembly. *Koch* et al. [41.161] used self-assembled wax platelets on artificial substrates and a lost wax casting process to transfer the platelet structures into artificial resin (Spurr's resin) surfaces. Another fast and low-cost technique to develop superhydrophobic surfaces is molding of hierarchical leaf surfaces, based on which a fast nanostructure replication method for water-containing biomaterial has been developed. The technique is based on three production steps:

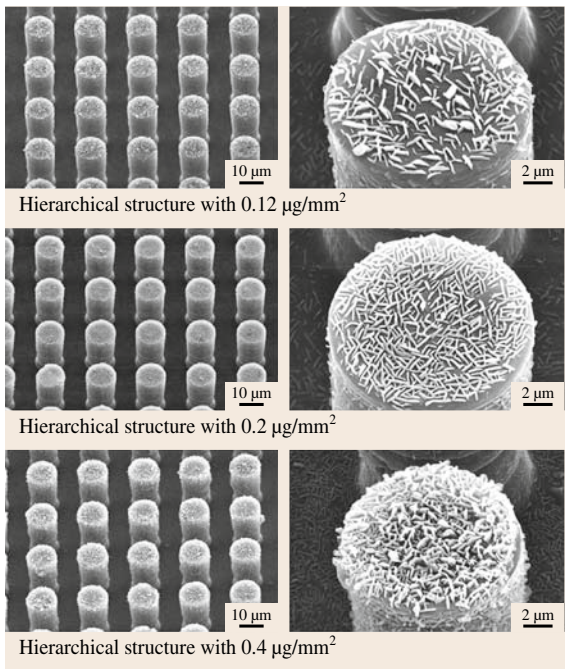

Fig. 41.25 Superhydrophobicity by hierarchical surfaces. SEM micrographs show replicated microstructured silicon surfaces with pillars of 14 µm diameter, 30 µm height, and 23 µm pitch, modified with self-assembled alkanes (hexatriacontane). From top to bottom an increase in crystal density is shown. The highest water repellency and lowest hysteresis has been found for the structures in the center, where 20 µg/cm² hexatriacontane was applied to the surfaces. These surfaces have been used for detailed study of wetting and adhesion (after [41.55])

1. Molding of a master surface
2. Removal of residues, such as wax crystals, from the mold
3. Filling of the mold with epoxy resin [41.162]

With this technique hierarchical structures of lotus leaves have been replicated and used for microscopy analysis and characterization of different properties, such as wettability and adhesion [41.4].

Superhydrophobic hierarchical surface structures can also be made by a combination of top-down and bottom-up techniques. One example is molding and multiple replication of artificial microstructured master surfaces and subsequent modification of the surfaces with self-assembling wax compounds or complete mixtures of plant waxes. For surface modification and homogenous covering of substrate surfaces with small three-dimensional crystalline nanostructures, thermo-evaporation of long-chain hydrocarbons has been used [41.162]. With this technique different molecules can be used to develop different nanostructure morphologies. Crystal sizes can be varied by changing the time of crystal growth, and the density of crystals on the surface can be controlled by the amount of evaporated material. We used this method to modify the nanostructures of replicated microstructured silicon surfaces for detailed wetting and adhesion analysis. Optimized hierarchical surface structures for self-cleaning approaches have been developed by replication of microstructured silicon surfaces and alkane and wax tubule self-assembly (Fig. 41.25). The optimized surfaces show contact angles above 170° and very low hysteresis of $\approx 2°$ tilting angle and therefore comply with the requirements for self-cleaning surfaces. The results of these studies are shown in [41.54, 55, 163].

41.3.4 Existing and Potential Use of Superhydrophobic Surfaces

Self-Cleaning Superhydrophobic Surfaces

Inspired by the self-cleaning behavior of lotus leaves, various artificial superhydrophobic self-cleaning surfaces have been prepared by creating appropriate surface morphology and roughness. A patent on technical micro- and nanostructured self-cleaning surfaces was assigned to *Barthlott* [41.164]. Based on this the trademark lotus-effect has been introduced, and several industrial manufactures have developed first products, labeled with the lotus-effect trademark. The first product available was a façade paint named lotusan, which has been successfully on the market since 1999. Sprays for temporary covering of surfaces create a superhydrophobic film on artificial surfaces and can, if no longer required, simply be removed by wiping. Self-cleaning glasses have been installed in sensors of traffic control units on German autobahns, and the introduction of building textiles, including awnings, tents, and flags, is to be expected. The list of applications for external surfaces includes lacquers for vehicles [41.165, 166], waterproofing of clothes [41.167] and other textiles [41.168, 169], plastics [41.170], roof tiles [41.171], temporary coatings [41.172], and plastics for microfluidics. However, some existing products are only easy to clean. These surfaces have very low surface energies and are smooth on the microscale. They are superhydrophobic, but the movement of water cannot remove adhering particles from them.

There are only two mechanisms which lead to the self-cleaning property of surfaces. First is the described superhydrophobic double-structured surface, as described for the lotus leaf. The second is a photocatalytic hydrophilic surface. In this, titanium dioxide is present in the outermost surface layer, which disintegrates any adhering organic materials. An application of these functional surfaces is, for example, roof tiles or glasses.

The use of self-cleaning surfaces is limited by the micro- and nanoscale of the surface structures, which requires low wear for the maintenance of the material functionality; thus materials must either be very wear resistant or uses must involve low friction [41.173]. For self-cleaning, movement is required and exterior applications where surfaces are exposed to rain or where surfaces can be artificially sprayed with water are preferred. Self-cleaning surfaces have limited success in glass materials, because surface microstructures affect the diffraction of light and thus change the optical properties of, e.g., lenses. For integration of superhydrophobicity and transparency within the same surface, the dimensions of the roughness should be lower than the wavelength of visible light (ca. 380–760 nm) [41.124].

Superhydrophobicity for Underwater Use

The surfaces of a number of floating plants and semi-aquatic animals provide technical solutions for the design of underwater air-trapping surfaces, and some have recently been successfully transferred to technical prototypes [41.78, 79].

Solga et al. [41.78] and *Cerman* et al. [41.79] studied the morphology and capacity for air retention of the surfaces of several species of the floating water fern

Salvinia. These leaves are characterized by multicellular hairs with coverage of small three-dimensional waxes (Figs. 41.16 and 41.17) and are able to retain air films underwater for up to 17 days. For technical surfaces, the advantage of staying dry underwater is the reduction of drag during movement. A small layer of air on a superhydrophobic surface reduces friction drag by 80% at a speed of 4 m/s and by 55% at 8 m/s [41.174, 175]. *Solga* et al. [41.78] list five surface characteristics as crucial for a stable, long-lasting underwater air film:

1. Hydrophobicity
2. Hairs with lengths of a few micrometers to several millimeters
3. Additional fine structures such as ridges, hairs or waxes
4. Micro- and nanocavities
5. Elasticity of the structures

Based on these, a textile prototype which stays dry for about 4 days when submerged in water has been developed. *Cerman* et al. [41.79] performed experiments with biological templates of different *Salvinia* species and showed that these biomimetic surfaces are able to retain an air film underwater for 4 days. A patent for air-retaining surfaces, outlining different fields of application, such as textiles, varnishes, and coatings, has been submitted by *Cerman* et al. [41.176]. However, *Cerman* et al. [41.79] discuss that it is obvious that even hairy superhydrophobic surfaces alone cannot stay permanently dry underwater and suggest that the solution will lie in a combination of microbubble technology (a technique in which the air layer is permanently refilled) and optimization of air-retaining superhydrophobic surfaces.

Underwater superhydrophobicity might also be a solution for the reduction of accumulation of algae, bacteria, and other sessile marine organisms on underwater surfaces. Whether underwater superhydrophobic surfaces are a solution against marine fouling has recently been discussed in a review by *Genzer* and *Efimenko* [41.177]. They present the implications of superhydrophobicity for marine fouling and potential designs of coatings and roughness on multiple length scales, which are assumed to represent a new and promising platform for fabrication-efficient foul-release marine coatings. However, it seems that some work still needs to be done to fully understand the phenomenon of the different mechanisms of adhesion by different marine organisms.

41.4 Conclusions

The diversity of plant surface structures is a result of several million years of evolutionary processes, through which nature has developed and proved surface structures and their functions. As a result of this, different highly functional surfaces have been developed. Plants developed surfaces with dense layers of hairs and surface waxes for light reflection and the absorption of harmful UV radiation. Anti-adhesive surfaces have been developed by some carnivorous plants to catch small insects. Such anti-adhesive surfaces are built either by epicuticular waxes or by a hydrophilic surface, covered with a water film. In plants, superhydrophobic surfaces are formed by microstructured cells with three-dimensional waxes on them, or by multicellular hairs, which are also covered by three-dimensional waxes. Hierarchical roughness in the first type of plant surface leads to self-cleaning, however droplets sit on top of hairs in the second type of plants and do not provide self-cleaning of particles trapped between the hair, although air can be retained by this structures effectively. Some plants developed superhydrophilic, hairy or porous surfaces, for the uptake of water and nutrients. The given examples show that the cuticle and its hydrophobic waxes represent a multifunctional boundary layer. In this, the surface functionality is predominantly influenced by the occurrence of epicuticular waxes. These waxes represent a hydrophobic covering for the primary surfaces of nearly all land-living plants. Waxes mainly function as a transport barrier, but on many plants waxes form small three-dimensional crystals, which provide the structural basis for superhydrophobicity, light refection, adsorption of UV radiation, and the creation of anti-adhesive surfaces. The three-dimensional wax crystals originate by self-assembly of mainly alkane molecules and their derivates (alcohols, esters, and others). These molecules can be used to develop biomimetic surfaces with superhydrophobic, self-cleaning, and anti-adhesive properties. However, impressive new techniques and materials have been developed in recent years to develop superhydrophobic and self-cleaning surfaces after the model plant

lotus (*Nelumbo nucifera*). The superhydrophobic surfaces of the water fern *Salvinia* retain an air layer under water over several days. This surface property has been used to develop air-retaining biomimetic surfaces with potential use for underwater materials, e.g., for drag reduction on surfaces moving in water. It is to be expected that more biomimetic materials will be developed in the future, and the functional plant surface structures presented here might further stimulate research in biomimicry.

References

41.1 K. Koch, B. Bhushan, W. Barthlott: Diversity of structure, morphology and wetting of plant surfaces, Soft Matter **4**, 1799–1804 (2008)

41.2 K. Koch, B. Bhushan, W. Barthlott: Multifunctional surface structures of plants: An inspiration for biomimetics, Prog. Mater. Sci. **54**, 137–178 (2009)

41.3 K. Koch, I.C. Blecher, G. König, S. Kehraus, W. Barthlott: The superhydrophilic and superoleophilic leaf surface of *Ruellia devosiana* (*Acanthaceae*): A biological model for spreading of water and oil on surfaces, Funct. Plant Biol. **36**, 339–350 (2009)

41.4 K. Koch, B. Bhushan, Y.C. Jung, W. Barthlott: Fabrication of artificial Lotus leaves and significance of hierarchical structure for superhydrophobicity and low adhesion, Soft Matter **5**, 1386–1393 (2009)

41.5 M. Riederer, L. Schreiber: Protecting against water loss: analysis of the barrier properties of plant cuticles, J. Exp. Bot. **52**, 2023–2032 (2001)

41.6 W. Barthlott, C. Neinhuis: The purity of sacred lotus or escape from contamination in biological surfaces, Planta **202**, 1–8 (1997)

41.7 H. Bargel, K. Koch, Z. Cerman, C. Neinhuis: Structure-function relationships of the plant cuticle and cuticular waxes – A smart material?, Funct. Plant. Biol. Evans Rev. Ser. **3**, 893–910 (2006)

41.8 P. Kenrick, P.R. Crane: The origin and early evolution of plants on land, Nature **389**, 33–39 (1997)

41.9 P.J. Holloway: Section I – Reviews. Plant cuticles: Physiochemical characteristics and biosynthesis. In: *Air Pollutants and the Leaf Cuticle*, ed. by K.E. Percy, J.N. Cape, R. Jagels, C.J. Simpson (Springer, Berlin Heidelberg 1994)

41.10 P.E. Kolattukudy: Polyesters in higher plants, Adv. Biochem. Eng. Biotechnol. **71**, 4–49 (2001)

41.11 C.E. Jeffree: The fine structure of the plant cuticle. In: *Biology of the Plant Cuticle*, ed. by M. Riederer, C. Müller (Blackwell, Oxford 2006) pp. 11–125

41.12 J.T. Martin, B.E. Juniper: *The Cuticles of Plants* (Edward Arnold, London 1970)

41.13 D.F. Cutler, K.L. Alvin, C.E. Price (Eds.): *The Plant Cuticle* (Academic Press, London 1982)

41.14 G. Kerstiens: *Plant cuticles: an integrated functional approach* (BIOS Scientific Publishers, Oxford 1996)

41.15 M. Riederer, C. Müller: *Biology of the Plant Cuticle* (Blackwell, Oxford 2006)

41.16 M. Riederer, L. Schreiber: Waxes – The transport barriers of plant cuticles. In: *Waxes: Chemistry, Molecular Biology and Functions*, ed. by R.J. Hamilton (The Oily Press, Dundee 1995) pp. 131–156

41.17 C. Neinhuis, W. Barthlott: Characterization and distribution of water-repellent, self-cleaning plant surfaces, Ann. Bot. **79**, 667–677 (1997)

41.18 R. Fürstner, W. Barthlott, C. Neinhuis, P. Walzel: Wetting and self-cleaning properties of artificial superhydrophobic surfaces, Langmuir **21**, 956–961 (2005)

41.19 L.Q. Ren, S.J. Wang, X.M. Tian, Z.W. Han, L.N. Yan-Qiu, Z.M. Qiu: Non-smooth morphologies of typical plant leaf surfaces and their anti-adhesion effects, J. Bionic Eng. **4**, 33–40 (2007)

41.20 H. Bargel, C. Neinhuis: Tomato (*Lycopersicon esculentum* Mill.) fruit growth and ripening as related to the biomechanical properties of fruit skin and isolated cuticle, J. Exp. Bot. **56**, 1049–1060 (2005)

41.21 H.G. Edelmann, C. Neinhuis, H. Bargel: Influence of hydration and temperature on the rheological properties of plant cuticles and their impact on plant organ integrity, J. Plant Growth Regul. **24**, 116–126 (2005)

41.22 M. Riederer, K. Markstädter: Cuticular waxes: A critical assessment of current knowledge. In: *Plant Cuticles – An Integrated Functional Approach* (BIOS Scientific, Oxford 1996) pp. 189–198

41.23 L. Kunst, A.L. Samuels: Biosynthesis and secretion of plant cuticular wax, Prog. Lipid Res. **42**, 51–80 (2003)

41.24 R. Jetter, S. Schäffer: Chemical composition of the Prunus laurocerasus leaf surface. Dynamic changes of the epicuticular wax film during leaf development, Plant Phys. **126**, 1725–1737 (2001)

41.25 R. Jetter, L. Kunst, A.L. Samuels: Composition of plant cuticular waxes, Annu. Plant Rev. **23**, 145–175 (2006)

41.26 E.A. Baker: Chemistry and morphology of plant epicuticular waxes. In: *The Plant Cuticle*, ed. by D.F. Cutler, K.L. Alvin, C.E. Price (Academic, London 1982) pp. 139–165

41.27 T. Shepherd, D.W. Griffiths: The effects of stress on plant cuticular waxes, New Phytol. **171**, 469–499 (2006)

41.28 K. Koch, K.D. Hartmann, L. Schreiber, W. Barthlott, C. Neinhuis: Influence of air humidity on epicuticular wax chemical composition, morphology and

wettability of leaf surfaces. Env. Exp. Bot. **56**, 1–9 (2006)
41.29 C. Markstädter, W. Federle, R. Jetter, M. Riederer, B. Hölldobler: Chemical composition of the slippery epicuticular wax blooms on *Macaranga* (*Euphorbiaceae*) ant-plants, Chemoecology **10**, 33–40 (2000)
41.30 M. Riedel, A. Eichner, R. Jetter: Slippery surfaces of carnivorous plants: Composition of epicuticular wax crystals in *Nepenthes alata* Blanco pitchers, Planta **218**, 87–97 (2003)
41.31 M. Wen, C. Buschhaus, R. Jetter: Nanotubules on plant surfaces: Chemical composition of epicuticular wax crystals on needles of *Taxus baccata* L, Phytochemistry **67**, 1808–1817 (2007)
41.32 H. Ensikat, C. Neinhuis, W. Barthlott: Direct access to plant epicuticular wax crystals by a new mechanical isolation method, Int. J. Plant Sci. **161**, 143–148 (2000)
41.33 H.J. Ensikat, M. Boese, W. Mader, W. Barthlott, K. Koch: Crystallinity of plant epicuticular waxes: Electron and X-ray diffraction studies, Chem. Phys. Lipids **144**, 45–59 (2006)
41.34 W. Barthlott, C. Neinhuis, D. Cutler, F. Ditsch, I. Meusel, I. Theisen, H. Wilhelmi: Classification and terminology of plant epicuticular waxes, Bot. J. Linn. Soc. **126**, 237–260 (1998)
41.35 N.D. Hallam, B.E. Juniper: The anatomy of the leaf surface. In: *The Ecology of Leaf Surface Microorganisms*, ed. by T.F. Preece, C.H. Dickinson (Academic, London 1971) pp. 3–37
41.36 C.E. Jeffree, E.A. Baker, P.J. Holloway: Ultrastructure and recrystallization of plant epicuticular waxes, New Physiol. **75**, 539–549 (1975)
41.37 K. Koch, C. Neinhuis, H.J. Ensikat, W. Barthlott: Self assembly of epicuticular waxes on plant surfaces investigated by atomic force microscopy (AFM), J. Exp. Bot. **55**, 711–718 (2004)
41.38 K. Koch, H.J. Ensikat: The hydrophobic coatings of plant surfaces: epicuticular wax crystals and their morphologies, crystallinity and molecular self-assembly, Micron **39**, 759–772 (2008)
41.39 P.J. Holloway, C.E. Jeffree, E.A. Baker: Structural determination of secondary alcohols from plant epicuticular waxes, Phytochemistry **15**, 1768–1770 (1976)
41.40 R. Jetter, M. Riederer: In vitro reconstitution of epicuticular wax crystals: Formation of tubular aggregates by long chain secondary alkendiols, Bot. Acta **108**, 111–120 (1995)
41.41 W. Barthlott, I. Theisen, T. Borsch, C. Neinhuis: Epicuticular waxes and vascular plant systematics: Integrating micromorphological and chemical data. In: *Deep Morphology: Toward a Renaissance of Morphology in Plant Systematics*, Regnum Vegetabile, Vol. 141, ed. by T.F. Stuessy, V. Mayer, E. Hörandl (Gantner Verlag Ruggell/Liechtenstein 2003) pp. 189–206
41.42 I. Meusel, C. Neinhuis, C. Markstädter, W. Barthlott: Chemical composition and recrystallization of epicuticular waxes: coiled rodlets and tubules, Plant Biol. **2**, 1–9 (2000)
41.43 I. Meusel, C. Neinhuis, C. Markstädter, W. Barthlott: Ultrastructure, chemical composition and recrystallisation of epicuticular waxes: transversely ridged rodlets, Can. J. Bot. **77**, 706–720 (1999)
41.44 International Union of Crystallography: Report of the executive committee for 1991, Acta Crystalogr. A **48**, 922–946 (1992)
41.45 R. Jetter, M. Riederer: Epicuticular crystals of nonacosan-10-ol: In-vitro reconstitution and factors influencing crystal habits, Planta **195**, 257–270 (1994)
41.46 K. Koch, W. Barthlott, S. Koch, A. Hommes, K. Wandelt, W. Mamdouh, S. De-Feyter, P. Broekmann: Structural analysis of wheat wax (*Triticum aestivum*): From the molecular level to three dimensional crystals, Planta **223**, 258–270 (2006)
41.47 K. Koch, A. Dommisse, W. Barthlott: Chemistry and crystal growth of plant wax tubules of Lotus (*Nelumbo nucifera*) and Nasturtium (*Tropaeolum majus*) leaves on technical substrates, Cryst. Growth Des. **6**, 2571–2578 (2006)
41.48 J.M. Benyus: *Biomimicry: Innovation Inspired by Nature*, 2nd edn. (H. Collins Pub., New York 2002)
41.49 G.M. Whitesides, M. Boncheva: Beyond molecules: Self-assembly of mesoscopic and macroscopic components, Proc. Natl. Acad. Sci. USA **99**(8), 4769–4774 (2002)
41.50 J. Zhang, W. Zhong-Lin, J. Liu, C. Shaowei, G. Liu: *Self Assembled Nanostructures* (Kluwer Academic, New York 2003)
41.51 N. Boden, P.J.B. Edwards, K.W. Jolley: Self-assembly and self-organization in micellar liquid crystals. In: *Structure and Dynamics of Strongly Interacting Colloids and Supermolecular Aggregates in Solutions*, ed. by S.H. Chen, J.S. Huang, P. Tartaglia (Kluwer, Dordrecht 1992)
41.52 C. Neinhuis, K. Koch, W. Barthlott: Movement and regeneration of epicuticular waxes through plant cuticles, Planta **213**, 427–434 (2001)
41.53 D. Dorset: Development of lamellar structures in natural waxes – An electron diffraction investigation, J. Phys. D **32**, 1276–1280 (1999)
41.54 B. Bhushan, K. Koch, Y.C. Jung: Biomimetic hierarchical structure for self-cleaning, Appl. Phys. Lett. **93**, 093101 (2008)
41.55 B. Bhushan, K. Koch, Y.C. Jung: Nanostructures for superhydrophobicity and low adhesion, Soft Matter **4**, 1799–1804 (2008)
41.56 S. De Feyter, F.C. De Schryver: Self-assembly at the liquid/solid interface: STM reveals, J. Phys. Chem. B **109**, 4290–4302 (2005)
41.57 F.C. Meldrum, S. Ludwigs: Template-directed control of crystal morphologies, Macromol. Biosci. **7**, 152–162 (2007)

41.58 A. Dommisse: Self-assembly and pattern formation of epicuticular waxes on plant surfaces. Ph.D. Thesis (Rheinische Friedrich-Wilhelms Universität, Bonn 2007)

41.59 W. Barthlott, N. Ehler: *Rasterelektronenmikroskopie der Epidermis-Oberflächen von Spermatophyten, Tropische und subtropische Pflanzenwelt* (Akademie der Wissenschaften und Literatur/Franz Steiner, Mainz/Wiesbaden 1977), in German

41.60 W. Barthlott: Scanning electron microscopy of the epidermal surface in plants. In: *Scanning Electron Microscopy in Taxonomy and Functional Morphology*, ed. by D. Claugher (Clarendon Press, Oxford 1990) pp. 69–94

41.61 C. Martin, B.J. Glover: Functional aspects of cell patterning in aerial epidermis, Curr. Opin. Plant Biol. **10**, 70–82 (2007)

41.62 C.A. Brewer, W.K. Smith, T.C. Vogelmann: Functional interaction between leaf trichomes, leaf wettability and the optical properties of water droplets, Plant Cell Environ. **14**, 955–962 (1991)

41.63 G.J. Wagner, E. Wang, R.W. Shephers: New approaches for studying and exploiting an old protuberance, the plant trichome, Ann. Bot. **93**, 3–11 (2004)

41.64 E. Rodriguez, P.L. Healey, I. Mehta: *Biology and Chemistry of Plant Trichomes* (Plenum, New York 1984)

41.65 H.D. Behnke: Plant trichomes – structure and ultrastructure: General terminology, taxonomic applications, and aspects of trichome bacterial interaction in leaf tips of *Dioscorea*. In: *Biology and chemistry of plant trichomes*, ed. by E. Rodriguez, P.L. Healey, I. Mehta (Plenum Press, New York 1984) pp. 1–21

41.66 W. Barthlott, D. Hunt: Seed-diversity in *Cactaceae* subfam. *Cactoideae*. In: *Succulent Plant Research*, Vol. 5, ed. by D. Hundt (Milborne Port, England 2000)

41.67 P.G. Kevan, M.A. Lanet: Flower petal microtexture is a tactile cue for bees, Proc. Natl. Acad. Sci. USA **82**, 4750–4752 (1985)

41.68 R. Maheshwari: A scourge of mankind: From ancient times into the genomics era, Curr. Sci. **93**, 1249–1256 (2007)

41.69 H.C. Hoch, R.C. Staples, B. Whitehead, J. Comeau, E.D. Wolf: Signaling for growth orientation and cell differentiation by surface topography, Uromyces Sci. **239**, 1659–1663 (1987)

41.70 L.H.P. Jones, K.A. Handreck: Silica in soils, plants, and animals, Adv. Agron. **19**, 107–149 (1967)

41.71 A.G. Sangster, M.J. Hodson, H.J. Tubb: Silicon deposition in higher plants. In: *Silicon in Agriculture*, ed. by L.E. Datnoff, G.H. Snyder, G.H. Korndörfer (Elsevier, Amsterdam 2001) pp. 85–114

41.72 F. Fauteux, W. Remus-Borel, J.G. Menziesb, R.R. Belanger: Silicon and plant disease resistance against pathogenic fungi, FEMS Microbiol. Lett. **249**, 1–6 (2005)

41.73 R.K. Saeedur: *Calcium Oxalate in Biological Systems* (CRC, Boca Raton 1995) p. 375

41.74 V.R. Franceschi, P.A. Nakata: Calcium oxalate in plants: Formation and function, Annu. Rev. Plant Biol. **56**, 41–71 (2005)

41.75 A. Fahn: Structure and function of secretory cells, Adv. Bot. Res. **31**, 37–75 (2000)

41.76 E. Wollenweber: The distribution and chemical constituents of the farinose exudates in gymnogrammoid ferns, Am. Fern. J. **68**, 13–28 (1978)

41.77 W. Barthlott, E. Wollenweber: Zur Feinstruktur, Chemie und Taxonomischen Signifikanz Epicuticularer Wachse und ähnlicher Sekrete, Trop. Subtrop. Pflanzenwelt **32**, 7–67 (1981), in German

41.78 A. Solga, Z. Cerman, B.F. Striffler, M. Spaeth, W. Barthlott: The dream of staying clean: Lotus and biomimetic surfaces, Bioinspir. Biomimetics **2**, 1–9 (2007)

41.79 Z. Cerman, B.F. Striffler, W. Barthlott: Dry in the water: The superhydrophobic water fern *Salvinia* – A model for biomimetic surfaces. In: *Functional Surfaces in Biology: Little Structures with Big Effects*, Vol. I, ed. by S.N. Gorb (Springer, Berlin Heidelberg 2009)

41.80 W. Barthlott, S. Wiersch, Z. Colic, K. Koch: Classification of trichome types within the water ferns *Salvinia* and ontogeny of the eggbeater trichomes, Botany **87**, 830–836 (2009)

41.81 H.G. Jones, E. Rotenberg: Energy, radiation and temperature regulation in plants. In: *Encyclopedia of Life Sciences* (Wiley, New York 2001) pp. 1–8 (2001)

41.82 D.M. Gates: Transpiration and leaf temperature, Ann. Rev. Plant Phys. **19**, 211–238 (1968)

41.83 D.M. Gates: Energy exchange and transpiration. In: *Water and Plant Life*, Ecological Studies, Vol. 19, ed. by O.L. Lange, L. Kappen, E.D. Schulze (Springer, New York 1976) pp. 137–147

41.84 P.H. Schuepp: Model experiments on free convection heat and mass transfer of leaves and plant elements, Bound.-Layer Meteorol. **3**, 454–457 (1973)

41.85 P.H. Schuepp: Leaf boundary layers, New Phytol. **125**, 477–507 (1993)

41.86 P.S. Nobel: *Physicochemical and Environmental Plant Physiology* (Academic, San Diego 1991)

41.87 M. Riederer: The cuticles of conifers: Structure, composition and transport properties. In: *Forest Decline and Air Pollution: A study of spruce (Picea abies) on acid soil*, Ecological Studies, Vol. 77, ed. by E.D. Schulze, O.L. Lange, R. Oren (Springer, Berlin Heidelberg 1989), pp. 157–192

41.88 R.H. Grant, G.M. Heisler, W. Gao, M. Jenks: Ultraviolet leaf reflectance of common urban trees and the prediction of reflectance from leaf surface

characteristics, Agric. For. Meteorol. **120**, 127–139 (2003)
41.89 J.D. Barnes, J. Cardoso-Vilhena: Interactions between electromagnetic radiation and the plant cuticle. In: *Plant Cuticles, an integrated approach*, ed. by G. Kerstiens (BIOS Scientific, Oxford 1996) pp. 157–170
41.90 M.G. Holmes, D.R. Keiller: Effects of pubescence and waxes on the reflectance of leaves in the ultraviolet and photosynthetic wavebands: A comparison of a range of species, Plant Cell Env. **25**, 85–93 (2002)
41.91 E.E. Pfündel, G. Agati, Z.G. Cerovic: Optical properties of plant surfaces, Annu. Plant Rev. **3**, 216–239 (2006)
41.92 S. Robinson, C.E. Lovelock, C.B. Osmond: Wax as a mechanism for protection against photoinhibition: A study of *Cotyledon orbiculata*, Bot. Acta **106**, 307–312 (1993)
41.93 C. Müller, M. Riederer: Plant surface properties in chemical ecology, Chem. Ecol. **3**, 2621–2651 (2005)
41.94 R. Sinclair, D.A. Thomas: Optical properties of leaves of some species in arid South Australia, Austral. Bot. **18**, 261–273 (1970)
41.95 P. Krauss, C. Markstädter, M. Riederer: Attenuation of UV radiation by plant cuticles from woody species, Plant Cell Env. **20**, 1079–1085 (1997)
41.96 A.E. Stapleton, V. Walbot: Flavonoids can protect maize DNA from the induction of ultraviolet radiation damage, Plant Physiol. **105**, 881–889 (1994)
41.97 L.C. Olsson, M. Veit, J.F. Bornman: Epidermal transmittance and phenolics composition of atrazine-tolerant and atrazine-sensitive cultivars of *Brassica napus* grown under enhanced UV-B radiation, Phys. Plant **107**, 259–266 (1999)
41.98 E. Wollenweber, U.H. Dietz: Occurrence and distribution of free flavonoid aglycones in plants, Phytochemistry **20**, 869–932 (1981)
41.99 J.F. Jacobs, G.J.M. Koper, W.N.J. Ursem: UV protective coatings: A botanical approach, Prog. Org. Coat. **58**, 166–171 (2007)
41.100 J.R. Ehleringer, O. Björkman: Pubescence and leaf spectral characteristics in a desert shrub *Encelia farinosa*, Oecologia **36**, 151–162 (1978)
41.101 P.S. Nobel: *Biophysical Plant Physiology and Ecology* (Freeman, San Francisco 1983)
41.102 S.D. Eigenbrode: Plant surface waxes and insect behaviour. In: *Plant Cuticles: An Integrated Functional Approach*, ed. by G. Kerstiens (BIOS Scientific Publishers, Oxford 1996) pp. 201–222
41.103 R.G. Beutel, S.N. Gorb: Ultrastructure of attachment specializations of hexapods (*Arthropoda*): Evolutionary patterns inferred from a revised ordinal phylogeny, J. Zool. Syst. Evol. Res. **39**, 177–207 (2001)
41.104 S. Gorb: *Attachment Devises of Insect Cuticles* (Kluwer, Dortrecht 2001)
41.105 W. Federle, U. Maschwitz, B. Fiala, M. Riederer, B. Hölldobler: Slippery ant-plants and skilful climbers: Selection and protection of specific ant partners by epicuticular wax blooms in *Macaranga* (*Euphorbiaceae*), Oeco **112**, 217–224 (1997)
41.106 S. Poppinga: Pflanzen fangen Tiere: Mikroskopische Charakteristika von Gleitfallen. Diploma Thesis (Nees Institut for Biodiversity of Plants, Universtität Bonn 2007), in German
41.107 B.E. Juniper, R.J. Robins, D.M. Joel: *The Carnivorous Plants* (Academic, London 1989)
41.108 E. Gorb, K. Haas, A. Henrich, S. Enders, N. Barbakadze, S. Gorb: Composite structure of the crystalline epicuticular wax layer of the slippery zone in the pitchers of the carnivorous plant *Nepenthes alata* and its effect on the insect attachment, J. Exp. Biol. **208**, 4651–4662 (2005)
41.109 H. Bohn, W. Federle: Insect aquaplaning: *Nepenthes* pitcher plants capture prey with the peristome, a fully wettable water-lubricated anisotropic surface, Proc. Natl. Acad. Sci. USA **39**, 14138–14143 (2004)
41.110 U. Bauer, H.F. Bohn, W. Federle: Harmless nectar source or deadly trap: *Nepenthes* pitchers are activated by rain, condensation and nectar, Proc. R. Soc. B **275**, 259–265 (2008)
41.111 H.C. Flemming: Auswirkungen mikrobieller Materialzerstörung. In: *Mikrobielle Materialzerstörung*, ed. by H. Brill (Georg Fischer, Stuttgart 1995) pp. 15–23, in German
41.112 J.N. Israelachvili: *Intermolecular and Surface Forces*, 2nd edn. (Academic Press, London 1992)
41.113 B. Bhushan: *Introduction to Tribology* (Wiley, New York 2002)
41.114 P.G. De Gennes, F. Brochard-Wyart, D. Quere: *Capillarity and Wetting Phenomena: Drops, Bubbles, Pearls, Waves* (Springer, New York 2004)
41.115 B. Bhushan (Ed.): *Nanotribology and Nanomechanics – An Introduction*, 2nd edn. (Springer, Heidelberg 2008)
41.116 A.V. Adamson: *Physical Chemistry of Surfaces* (Wiley, New York 1990)
41.117 R.N. Wenzel: Resistance of solid surfaces to wetting by water, Ind. Eng. Chem. **28**, 988 (1936)
41.118 A.B.D. Cassie, S. Baxter: Wettability of porous surfaces, Trans Faraday Soc. **40**, 546 (1944)
41.119 M. Reyssat, J.M. Yeomans, D. Quere: Impalement of fakir drops, Europhys Lett. **81**, 26006 (2008)
41.120 Y.C. Jung, B. Bhushan: Wetting behavior during evaporation and condensation of water microdroplets on superhydrophobic patterned surfaces, J. Microsc. **229**, 127–140 (2008)
41.121 C.W. Extrand: Model for contact angle and hysteresis on rough and ultraphobic surfaces, Langmuir **18**, 7991–7999 (2002)
41.122 B. Bhushan, Y.C. Jung: Wetting study of patterned surfaces for superhydrophobicity, Ultramicroscopy **107**, 1033–1041 (2007)

41.123 P. Roach, N.J. Shirtcliffe, M.I. Newton: Progress in superhydrophobic surface development, Soft Matter **4**, 224–240 (2008)

41.124 X. Zhang, F. Shi, J. Niu, Y. Jiang, Z. Wang: Superhydrophobic surfaces: from structural control to functional application, J. Mater. Chem. **18**, 621–633 (2008)

41.125 J. Heintzenberg: Fine particles in the global troposphere – A review, Tellus B **41**, 149–160 (1989)

41.126 J. Burkhardt, H. Kaiser, H. Goldbach, L. Kappen: Measurements of electrical leaf surface conductance reveal re-condensation of transpired water vapour on leaf surfaces, Plant Cell Environ. **22**, 189–196 (1999)

41.127 J. Burkhardt, K. Koch, H. Kaiser: Deliquescence of deposited atmospheric particles on leaf surfaces, Water Air Soil Pollut. **1**, 313–321 (2001)

41.128 W. Barthlott, W. Schultze-Motel: Zur Feinstruktur der Blattoberflächen und Systematischen Stellung der Laubmoosgattung *Rhacocarpus* und anderer *Hedwigiaceae*, Willdenowia **11**, 3–11 (1981), in German

41.129 H.G. Edelmann, C. Neinhuis, M. Jarvis, B. Evans, E. Fischer, W. Barthlott: Ultrastructure and chemistry of the cell wall of the moss *Rhacocarpus purpurascens* (*Rhacocarpaceae*): A puzzling architecture among plants, Planta **206**, 315–321 (1998)

41.130 A. Otten, S. Herminghaus: How plants keep dry: A physicist's point of view, Langmuir **20**, 2405–2408 (2004)

41.131 W.E. Ward: The lotus symbol: Its meaning in Buddhist art and philosophy, J. Aesthet. Art Crit. **11**, 135–146 (1952)

41.132 T.S. Chow: Nanoscale surface roughness and particle adhesion on structures substrates, Nanotechnology **18**, 1–4 (2007)

41.133 O. Pitois, X. Chateau: Small particle at a fluid interface: effect of contact angle hysteresis on force and work of detachment, Langmuir **18**, 9751–9756 (2002)

41.134 B. Bhushan, Y.C. Jung: Wetting, adhesion and friction of superhydrophobic and hydrophilic leaves and fabricated micro/nanopatterned surfaces, J. Phys.: Condens. Matter **20**, 225010 (2008)

41.135 A.K. Stosch, A. Solga, U. Steiner, C. Oerke, W. Barthlott, Z. Cerman: Efficiency of self-cleaning properties in wheat (*Triticum aestivum* L.), Appl. Bot. Food Qual. **81**, 49–55 (2007)

41.136 W. Barthlott, K. Riede, M. Wolter: Mimicry and ultrastructural analogy between the semi-aquatic grasshopper *Paulinia acuminata* (*Orthoptera: Pauliniidae*) and its foodplant, the water-fern *Salvinia auriculata* (*Filicatae: Salviniaceae*), Amazoniana **13**, 47–58 (1994)

41.137 M. Ayre: *Biomimicry – A review. Work package report, European Space Research & Technology Centre (ESTEC)* (European Space Agency (ESA), Noordwijk 2003)

41.138 D.W. Bechert, M. Bruse, W. Hage, R. Meyer: Fluid mechanics of biological surfaces and their technological application, Naturwissenschaften **87**, 157–171 (2000)

41.139 S.J. Abbott, P.H. Gaskell: Mass production of bio-inspired structured surfaces, Proc. Inst. Mech. Eng, Part C: J. Mech. Eng. Sci. **221**, 1181–1191 (2007)

41.140 H.C. Von Baeyer: The Lotus effect, The Sciences **40**, 12–15 (2000)

41.141 P. Forbes: *The Gecko's Foot* (Fourth Estate, London 2005)

41.142 A.K. Geim, S.V. Dubonos, I.V. Grigorieva, K.S. Novoselov, A.A. Zhukov, S.Y. Shapoval: Microfabricated adhesive mimicking gecko foot-hair, Nat. Mater. **2**, 461–463 (2003)

41.143 S. Gorb, M. Varenberg, A. Peressadko, J. Tuma: Biomimetic mushroom-shaped fibrillar adhesive microstructures, J. R. Soc. Interface **4**, 271–275 (2007)

41.144 B. Bhushan, R.A. Sayer: Surface characterization and friction of a bio-inspired reversible adhesive tape, Microsyst. Technol. **13**, 71–78 (2007)

41.145 M. Zhang, M. Liu, H. Prest, S. Fischer: Nanoparticles secreted from ivy rootlets for surface climbing, Nano Lett. **8**, 1277–1280 (2008)

41.146 T. Speck, T. Masselter, B. Prüm, O. Speck, R. Luchsinger, S. Fink: Plants as concept generators for biomimetic light-weight structures with variable stiffness and self-repair mechanisms, J. Bionics Eng. **1**, 199–205 (2004)

41.147 Y. Bar-Cohen: *Biomimetics: Biologically Inspired Technologies* (CRC Press Book, New York 2006)

41.148 P. Wagner, R. Fürstner, W. Barthlott, C. Neinhuis: Quantitative assessment to the structural basis of water repellency in natural and technical surfaces, J. Exp. Bot. **54**, 1295–1303 (2003)

41.149 Y.T. Cheng, D.E. Rodak, C.A. Wong, C.A. Hayden: Effects of micro- and nano-structures on the self-cleaning behaviour of lotus leaves, Nanotechnology **17**, 1359–1362 (2006)

41.150 M. Nosonovsky, B. Bhushan: Hierarchical roughness optimization for biomimetic superhydrophobic surfaces, Ultramicroscopy **107**, 969–979 (2007)

41.151 C.W. Extrand: Modeling of ultralyophobicity: Suspension of liquid drops by a single asperity, Langmuir **21**, 10370–10374 (2005)

41.152 A. Marmur: Wetting on hydrophobic rough surfaces: To be heterogeneous or not to be?, Langmuir **19**, 8343–8348 (2003)

41.153 S. Wang, L. Jiang: Definition of superhydrophobic states, Adv. Mater. **19**, 3423–3424 (2007)

41.154 L. Feng, Y. Zhang, J. Xi, Y. Zhu, N. Wang, F. Xia, L. Jiang: Petal effect: A superhydrophobic state with high adhesive force, Langmuir **24**, 4114–4119 (2008)

41.155 W. Li, A.A. Amirfazli: Hierarchical structures for natural superhydrophobic surfaces, Soft Matter **4**, 462–466 (2008)

41.156 M. Nosonovsky, B. Bhushan: Hierarchical roughness makes superhydrophobic states stable, Microelectron. Eng. **84**, 382–386 (2007)

41.157 M. Nosonovsky, B. Bhushan: Multiscale friction mechanisms and hierarchical surfaces in nano and bio-tribology, Mater. Sci. Eng. R **58**, 162–193 (2007)

41.158 M. Nosonovsky, B. Bhushan: Roughness induced superhydrophobicity: A way to design non adhesive surfaces, J. Phys. D **20**, 225009 (2008)

41.159 M. Nosonovsky, B. Bhushan: Biologically inspired surfaces: Broadening the scope of roughness, Adv. Func. Mater. **18**, 843–855 (2008)

41.160 C.J. Brinker: Evaporation-induced self-assembly: Functional nanostructures made easy, Mater. Res. Bull. **29**, 631–640 (2004)

41.161 K. Koch, A. Dommisse, W. Barthlott, S. Gorb: The use of plant waxes as templates for micro- and nanopatterning of surfaces, Acta Biomater. **3**, 905–909 (2007)

41.162 K. Koch, A.J. Schulte, A. Fischer, S. Gorb, W. Barthlott: A fast, precise and low cost replication technique for nano- and high aspect ratio structures of biological and artifical surfaces, Bioinspir. Biomimetics **3**, 046002 (2008)

41.163 B. Bhushan, Y.C. Jung, A. Niemietz, K. Koch: Lotus-like biomimetic hierarchical structures developed by self-assembly of tubular plant waxes, Langmuir **25**, 1659–1666 (2009)

41.164 W. Barthlott: Self-cleaning surfaces of objects and process for producing same. Patent, EP 0772514 B1, 8, Germany (1998)

41.165 A. Born, J. Ermuth, C. Neinhuis: Fassadenfarbe mit Lotus-Effekt: Erfolgreiche übertragung bestätigt, Phänomen Farbe **2**, 34–36 (2000)

41.166 W. Ming, D. Wu, R. van Benthem, G. de With: Superhydrophobic films from raspberrylike particles, Nano Lett. **5**, 2298–2301 (2005)

41.167 H. Höcker: Plasma treatment of textile fibres, Pure Appl. Chem. **74**, 423–427 (2002)

41.168 L. Gao, T.J. McCarthy: "Artificial Lotus Leaf" prepared using a 1945 patent and a commercial textile, Langmuir **22**, 5998–6000 (2006)

41.169 M. Pociute, B. Lehmann, A. Vitkauskas: Wetting behaviour of surgerical polyester woven fabrics, Mater. Sci. **9**, 410–413 (2003)

41.170 E. Nun, M. Oles, B. Schleich: Lotus-Effect®-surfaces, Macromol. Symp. **187**, 677–682 (2002)

41.171 P. Dendl, J. Interwies: Method for imparting a self-cleaning feature to a surface, and an object provided with a surface of this type. Patent WO 2001/079141, Germany (2001)

41.172 F. Müller, P. Winter: Clean surfaces with the lotus-effect, J. Com. Esp. Deterg. **34**, 103–111 (2004)

41.173 M. Nosonovsky, B. Bhushan: *Multiscale Dissipative Mechanisms and Hierarchical Surfaces* (Springer, Berlin Heidelberg 2008)

41.174 J. Tokunaga, M. Kumada, Y. Sugiyama, N. Watanabe, Y.B. Chong, N. Matsubara: Method of forming air film on submerged surface of submerged part-carrying structure, and film structure on submerged surface, European Patent EP 0616940 (1993) pp. 1–14

41.175 K. Fukuda, J. Tokunaga, T. Nobunaga, T. Nakatani, T. Iwasaki, Y. Kunitake: Frictional drag reduction with air lubricant over a super-water-repellent surface, J. Marine Sci. Tech. **5**, 123–130 (2000)

41.176 Z. Cerman, B.F. Striffler, W. Barthlott, T. Stegmeier, A. Scherrieble, V. von Arnim: Superhydrophobe Oberflächen für Unterwasseranwendungen. Patent, DE 10 2006 009, (2006), in German

41.177 J. Genzer, K. Efimenko: Recent developments in superhydrophobic surfaces and their relevance to marine fouling: A review, Biofouling **22**, 339–360 (2006)